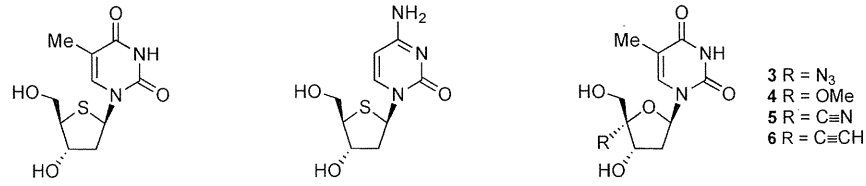

Figure 1. Structures of compounds **1**−**6**.

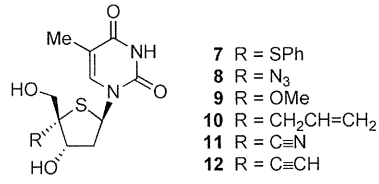

Figure 2. 4′-Substituted 4′-thiothymidines **7**−**12**.

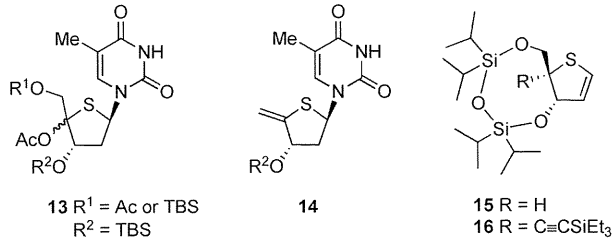

Figure 3. Structures of compounds **13**−**16**.

1-diazo(2-oxopropyl)phosphonate[8] to provide the ethynyl-substituted tetrahydrothiophene derivative **D**.

Compound **17** (Figure 4), which corresponds to the aldehyde **A** of Scheme 1, was prepared from 2,3-*O*-isopropylidene-L-lyxonolactone (**18**).[9] Namely, by following the reported procedures,[10] **18** was converted to the dimesylate **19**. Reaction of **19** with Na_2S in DMF at 80 °C led to the formation of the 1,4-anhydro-4-thio-D-ribitol derivative **20** in 66% overall yield from **18**. Compound **20** was desilylated with Bu_4NF to give **21** in 81% yield.[11] Finally, oxidation of **21** with IBX (2-iodoxybenzoic acid) in CH_3CN provided the aldehyde **17** in 83% yield.[12]

Subsequent aldol reaction between **17** and 37% aqueous formaldehyde was carried out in 60% aqueous dioxane (room temperature, overnight), and the resulting mixture was silylated with TBSCl. In the presence of K_2CO_3, the aldols **22** and **23** (Figure 5) were obtained in 21 and 13% yields, respectively, together with the silyl enol ether **24** (16%). The yield of the desired stereoisomer **22** was improved to 50% by using $NaHCO_3$, although the formation of **23** (18%) and **24** (14%) could not be eliminated.

The formyl group of **22** was converted to an ethynyl group through its reaction with dimethyl 1-diazo(2-oxopropyl)phosphonate in MeOH in the presence of K_2CO_3. Upon reacting the crude product with Bu_4NF, the 4-ethynyl derivative **25** was isolated in 73% yield from **22**.

Compound **25** was transformed to 4-thiofuranoid glycal **26** by reaction with *tert*-BuLi (4 equiv) at −70 °C in THF (Figure 6).[13] This reaction furnished the glycal **26** in 61% yield along with the ring-opened sulfide **27** (9%) and the starting material **25** (11%). The actual glycosyl donor **16** was prepared from **26** by first protecting the hydroxyl groups with the TIPDS group (yield of **28**, 72%) and then the ethynyl group with a triethylsilyl group (yield of **16**, 90%).

With the glycosyl donor **16** in hand, electrophilic glycosidation with a suitable nucleobase was examined. When **16** was reacted with N^4,O^2-bis-trimethylsily-N^4-acetylcytosine (1.5 equiv) in the presence of NIS (1.5 equiv) in CH_3CN/CH_2Cl_2 at room temperature overnight, the desired β-anomer **29** of the glycosidated product was formed as a single stereoisomer in 61% yield (Figure 7).[14] The depicted structure was confirmed by nuclear Overhauser effect (NOE) experiment: H-6/H-2′ (1%), H-6/H-3′ (5%), and H-6/CH_2-5′(0.2%). The observed exclusive formation of **29** suggested that the presence of the ethynyl group at the 4-position of 3,5-*O*-TIPDS-4-thiofuranoid glycal **15** does not influence the β-face selectivity of the electrophilic glycosidation.[7] The introduced iodine atom of **29** was removed by reaction with Bu_3SnH/Et_3B at −70 °C under an O_2 atmosphere to give **30** in 94% yield. To circumvent the difficult chromatographic separation of the free nucleoside and the side product derived from the silyl-protecting group, **30** was converted to its corresponding acetate **31** (99% isolated yield) by desilylation with Bu_4NF and subsequent acetylation in one pot. Finally, **31** was converted to the target 4′-ethynyl-2′-deoxy-4′-thiocytidine **32** (91% isolated yield) by treatment with K_2CO_3 in MeOH.

We next turned our attention to the synthesis of the adenine and guanine nucleosides. Under similar reaction conditions for the electrophilic glycosidation of N^4-acetylcytosine, bis-trimethylsilyl-N^6-benzoyladenine was reacted with **16**. In this reaction, the target nucleoside **33** could be obtained in 48% isolated yield as a single stereoisomer together with its regioisomers **34** (12%) and **35** (13%) (Figure 8).[15] The depicted structures of **33**−**35** were determined on the basis of comprehensive NMR studies including NOE, heteronuclear multiple quantum coherence, and heteronuclear multiple bond correlation experiments.[16] A similar regiochemical outcome was also observed in the glycosidation of N^2-acetyl-O^6-diphenylcarbamoylguanine,[17] where three isomeric nucleosides **36**−**38** were isolated in 25, 12, and 29% yields, respectively (Figure 9).

The N^9-glycosidated products **33** and **36** were successfully converted to 4′-ethynyl-4′-thio-2′-deoxyadenosine **41** and the respective guanosine nucleoside **43** by three steps as follows: (1) Bu_3SnH/Et_3B/PhMe, −70 °C (yield of **39**, 88%; yield of **42**, 72%), (2) Bu_4NF/Ac_2O/THF (yield of **40**, quant.), and (3) K_2CO_3/MeOH (yield of **41**, 82%; yield of **43**, 63% from **42** for two steps) (Figure 10).

The anti-HIV-1 activities of **32**, **41**, and **43** were evaluated, and the results are summarized in Table 1.[18,19] To compare the antiviral activity and cytotoxicity with the corresponding 4′-oxygen counterparts, reported biological data[20,21] of 4′-ethynyl derivatives of 2′-deoxycytidine **44**, 2′-deoxyadenosine **45**, and 2′-deoxyguanosine

dx.doi.org/10.1021/ml2001054 |ACS Med. Chem. Lett. 2011, 2, 692–697

Scheme 1. Introduction of an Ethynyl Group on a Tetrahydrothiophene Ring

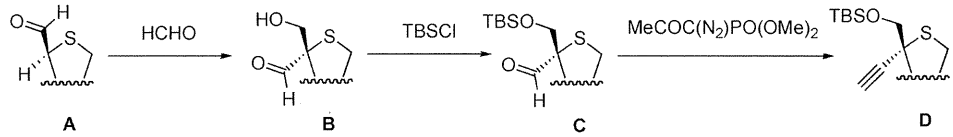

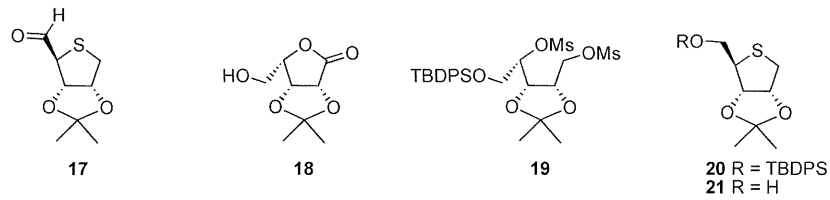

Figure 4. Structures of compounds **17**—**21**.

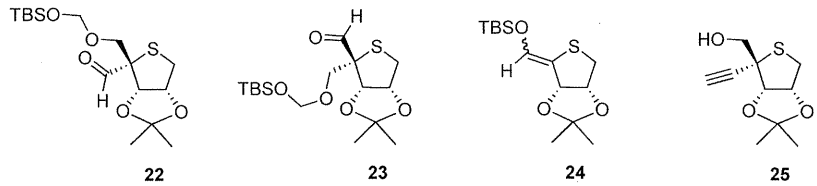

Figure 5. Structures of compounds **22**—**25**.

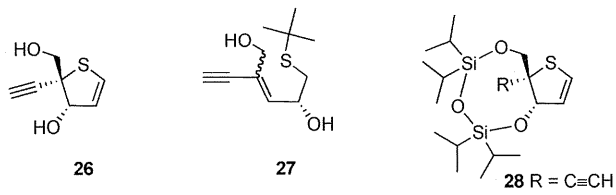

Figure 6. Structures of compounds **26**—**28**.

46 are also included in Table 1. As can be seen in entry 1, 4′-ethynyl-2′-deoxy-4′-thiocytidine **32** exhibited a 10 times lower inhibitory activity than that of the corresponding deoxycytidine derivative **44**. However, because **32** was less toxic to MT-4 cells, the SI value (545) of **32** was found to be comparable to that of **44** (458). In the case of adenine nucleosides as shown in entry 2, a similar trend was seen in terms of EC_{50} and CC_{50} values. In contrast, 4′-ethynyl-2′-deoxy-4′-thioguanosine **43** was found to be a highly promising anti-HIV agent (entry 3). Indeed, **43** exhibited comparable antiviral activity (EC_{50}: 0.0055 μM for **43** vs 0.0015 μM for **46**) and did not show any cytotoxicity to MT-4 cells up to 100 μM in contrast to the highly toxic 2′-deoxyguanosine derivative **46** (CC_{50}: 1.4 μM). The promising guanine nucleoside **43** possesses a SI value of >18200, which is 20 times better than that of 4′-ethynyl-2′-deoxyguanosine **46** (SI 933).

With the above promising anti-HIV-1 activity in hand, next, the 4′-substituted 2′-deoxy-4′-thioribonucleosides **32**, **41**, and **43** were also evaluated for their inhibitory activity against a series of other viruses including HSV-1 strain KOS, HSV-2 strain G, TK^- HSV-1 strain KOS resistant to ACV, and vaccinia virus Lederle strain, and the results were summarized in Table 2.[22] Antiviral data of ganciclovir are also included as a reference compound. As can be seen, these nucleoside derivatives also exhibited antiviral activity against herpes simplex virus and vaccinia virus without measurable cytotoxicity to the host cells up to 100 μM (entries 1—3). These potencies are at least 100 times less than that of ganciclovir, but their selectivity indices against HSV-1 and HSV-2 were >50—100 for **32** and **43**. However, it is noteworthy that all compounds synthesized in this study suppressed the replication of the thymidine kinase-deficient (TK^-) HSV-1 KOS strain at an almost equal potency as wild-type HSV-1. In contrast, the potency of ganciclovir against HSV-1 TK^- strain (1 μM) is 100-fold weaker as compared to wild-type HIV-1. These data are somewhat surprising but interesting and may suggest that the antiherpesvurus activity of **32**, **41**, and **43** is independent of the activation (phosphorylation) by the virus-encoded thymidine kinase. This may, in turn, point to another mechanism of antihepetic action of these compounds.

The compounds were not significantly inhibitory against other viruses, including parainfluenza virus, reovirus-1, Sindbis virus, Coxsackie virus B4, Punta Toro virus in Vero cell cultures, VSV and RSV in HeLa cell cultures, feline corona virus (FIPV) and feline herpesvirus in CrFK cell cultures, and influenza virus A (H1N1, H3N2) and B in MDCK cell cultures.

In conclusion, we have developed a novel synthetic approach to 4′-ethynyl-2′-deoxy-4′-thioribonucleosides on the basis of electrophilic glycosidation utilizing 4-ethynyl-4-thiofuranoid glycal **16** as a glycosyl donor. The synthesis of **16** was initiated with the β-face-selective aldol reaction of 1,4-anhydro-2,3-*O*-isopropylidene-4-thio-D-ribitol 5-aldehyde **17** with formaldehyde. The aldol **22** was reacted with dimethyl 1-diazo(2-oxopropyl)phosphonate to provide the ethynyl-substituted tetrahydrothiophene derivative **25**. 4-Ethynyl-4-thiofuranoid glycal **26** was obtained by the reaction of **25** with *tert*-BuLi. The actual glycosyl donor **16**

was prepared by silyl-protection of the hydroxyl and ethynyl groups of **26**.

The glycosidation between **16** and the silylated nucleobase (N^4-acetylcytosine, N^6-benzoyladenine, and N^2-acetyl-O^6-diphenylcarbamoylguanine) proceeded with facial selectivity and β-anomers

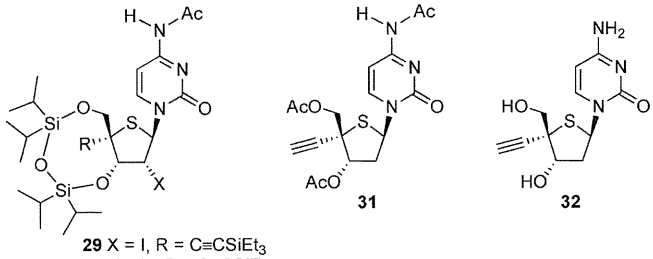

Figure 7. Structures of compounds **29**–**32**.

29, **33**, and **36** of the glycosidated products could be obtained exclusively. These glycosides were efficiently transformed into the 4′-ethynyl derivatives of 2′-deoxy-4′-thiocytidine (**32**), -adenosine (**41**), and -guanosine (**43**). It is noteworthy that these novel nucleoside analogues synthesized in this study were found to be less cytotoxic to MT-4 cells as compared to the corresponding 2′-deoxycytidine (**44**), 2′-deoxyadenosine (**45**), and 2′-deoxyguanosine (**46**) derivatives. By comparison with the reported SI value of 4′-ethynyl-2′-deoxyguanosine **46**, it was found that the SI for the 2′-deoxy-4′-thioguanosine derivative **43** has a 20-fold better value (>18200) than that of 2′-deoxyguanosine counterpart (933). These facts suggest that replacement of the furanose oxygen with sulfur atom is a promising approach for the development of less cytotoxic antiviral nucleosides. We are currently investigating the mechanism of the promising biological profile of these compounds.

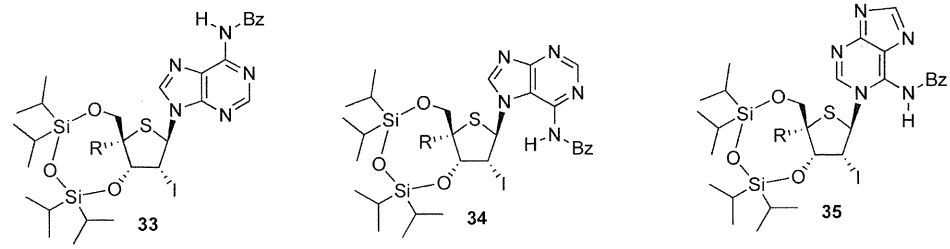

Figure 8. Structures of compounds **33**–**35** (R = C≡CSiEt$_3$).

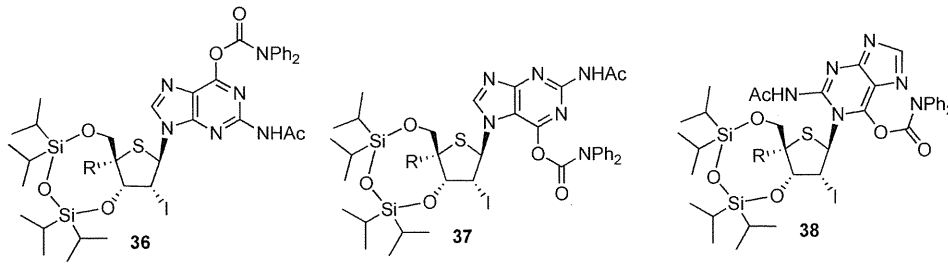

Figure 9. Structures of compounds **36**–**38** (R = C≡CSiEt$_3$).

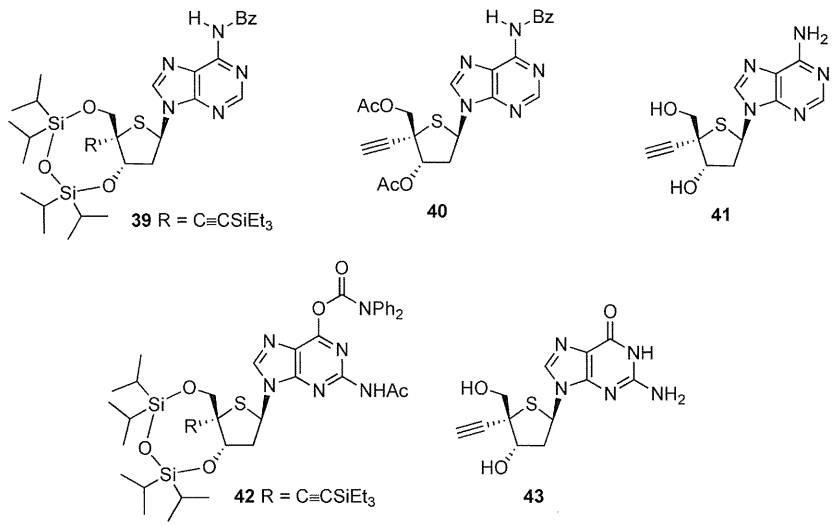

Figure 10. Structures of compounds **39**–**43**.

dx.doi.org/10.1021/ml2001054 |ACS Med. Chem. Lett. 2011, 2, 692–697

Table 1. Inhibitory Effect of 4′-Ethynyl-2′-deoxy-4′-thioribonucleosides (32, 41, and 43) and Its Oxygen Analogues (44–46) on HIV-1 in MT-4 Cells

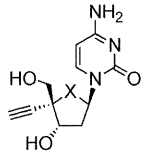

32: X = S
44: X = O

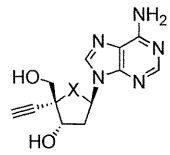

41: X = S
45: X = O

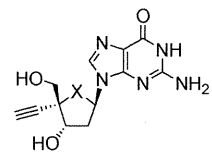

43: X = S
46: X = O

entry	compd	EC_{50} (μM)[a]	CC_{50}(μM)[b]	SI[c]	compd	EC_{50} (μM)[d]	CC_{50}(μM)[d]	SI [c]
1	**32**	0.011 ± 0.001	6.0 ± 1.2	545	**44**	0.0048 ± 0.001	2.2 ± 1.0	458
2	**41**	0.087 ± 0.017	>20	>230	**45**	0.0098 ± 0.0043	16 ± 7.9	1630
3	**43**	0.0055 ± 0.0016	>100	>18200	**46**	0.0015 ± 0.0003	1.4 ± 0.16	933

[a] Inhibitory concentration required to achieve 50% protection of MT-4 cells against the cytopathic effect of HIV-1. [b] Cytotoxic concentration required to reduce the viability of mock-infected MT-4 cells by 50%. [c] SI = CC_{50}/EC_{50} [d] Data taken from refs 20 and 21.

Table 2. Inhibitory Effect of 4′-Ethynyl-2′-deoxy-4′-thioribonucleosides (32, 41, and 43) against Herpes Simplex Virus and Vaccinia Virus in HEL Cell Cultures[a]

		EC_{50} (μM)[b]				
entry	compd	herpes simplex virus-1 (KOS)	herpes simplex virus-2 (G)	vaccinia virus	herpes simplex virus-1 (KOS, TK^- ACV)	minimum cytotoxic concentration[c] (μM)
1	**32**	2 ± 0	1.5 ± 0.5	6.5 ± 2.5	2.5 ± 0.5	>100
2	**41**	7 ± 5	4 ± 0	52 ± 6.0	8 ± 4.0	>100
3	**43**	3 ± 1	1.5 ± 0.5	27 ± 7.0	4.5 ± 2.5	>100
4	ganciclovir	0.01	0.01	100	1	>100

[a] Data derived from two independent experiments. [b] Required to reduce virus-induced cytopathogenicity by 50%. [c] Required to cause a microscopically detectable alternation of normal cell morphology.

■ ASSOCIATED CONTENT

Supporting Information. Experimental procedures and full characterization for compounds **16**–**17** and **20**–**43**. This material is available free of charge via the Internet at http://pubs.acs.org.

■ AUTHOR INFORMATION

Corresponding Author

*Tel: 81-3-3784-8187. Fax: 81-3-3784-8252. E-mail: harakazu@pharm.showa-u.acjp.

Funding Sources

C.-Y.C. is a Fellow for the National Foundation for Cancer Research (NFCR). Financial support from the Japan Society for the Promotion of Science (KAKENHI No. 21590123 to K.H.), the NIH (#AI-38204 to Y.-C.C.), and the K.U. Leuven (GOA No. 10/014 to J.B.) are gratefully acknowledged.

■ ACKNOWLEDGMENT

We are also grateful to Y. Odanaka and M. Matsubayashi (Center for Instrumental Analysis, Showa University) for technical assistance with NMR, MS, and elemental analyses.

■ REFERENCES

(1) For a review, see *Nucleosides and Nucleotides as Antitumor and Antiviral Agents*; Chu, C. K., Baker, D. C., Eds.; Plenum Press: New York, 1993.

(2) Ichikawa, E.; Kato, K. Sugar-modified nucleosides in past 10 years, a review. *Curr. Med. Chem.* **2001**, *8*, 385–423.

(3) *Modified Nucleosides in Biochemistry, Biotechnology and Medicine*; Herdewijn, P., Eds.; Wiley-VCH Verlag GmbH & Co. KGaA: Weinheim, 2008.

(4) For a review, see Yokoyama, M. Synthesis and biological activity of thionucleosides. *Synthesis* **2000**, 1637–1655.

(5) For a review, seeHayakawa, H.; Kohgo, S.; Kitano, K.; Ashida, N.; Kodama, E.; Mitsuya, H.; Ohrui, H. Potential of 4′-substituted nucleosides for the treatment of HIV-1. *Antiviral Chem. Chemother.* **2004**, *15*, 169–187.

(6) Haraguchi, K.; Shimada, H.; Tanaka, H.; Hamasaki, T.; Baba, M.; Gullen, E. A.; Dutschman, G. E.; Cheng, Y.-C. Synthesis and anti-HIV activity of 4′-substituted 4′-thiothymidines: A new entry based on nucleophilic substitution of the 4′-acetoxy group. *J. Med. Chem.* **2008**, *5*, 1885–1893.

(7) Haraguchi, K.; Takahashi, H.; Shiina, N.; Horii, C.; Yoshimura, Y.; Nishikawa, A.; Sasakura, E.; Nakamura, K. T.; Tanaka, H. Stereoselective synthesis of the β-anomer of 4′-thionucleosides based on electrophilic glycosidation to 4-thiofuranoid glycal. *J. Org. Chem.* **2002**, *67*, 5919–5927.

(8) Müller, S.; Liepold, B.; Roth, G. J.; Bestmann, H. An improved one-pot procedure for the synthesis of alkynes from aldehydes. *Synlett* **1996**, 521–522.

(9) For the preparation of **18** from D-ribose, see Batra, H.; Moriaty, R. M.; Penmasta, R.; Sharma, V.; Stanciuc, G.; Stazewski, J. P.; Tuladhar, S. M.; Walsh, D. A. A concise, efficient and production-scale synthesis of a protected L-lyxonolactone derivative: An important aldonolactone core. *Org. Process Res. Dev.* **2006**, *10*, 484–486.

(10) Jayakanthan, K.; Johnston, B. D.; Pinto, B. M. Stereoselective synthesis of 4′-selenonucleosides using the Pummerer glycosylation reaction. *Carbohydr. Res.* **2008**, *343*, 1790–1800.

(11) For another method for the synthesis of **21**, see Jeong, L. S.; Lee, H. W.; Jacobson, K. A.; Kim, H. O.; Shin, D. H.; Lee, J. A.; Gao, Z.-G.; Lu, C.; Diong, H. T.; Gunaga, P.; Lee, S. K.; Jin, D. Z.; Chun, M. W.; Moon, H. R. Structure-activity relationships of 2-chloro-N^6-substituted-4′-thioadenosine-5′-uronamides as highly potent and selective agonists at the human A_3 adenosine receptor. *J. Med. Chem.* **2006**, *49*, 273–281.

(12) For another method for the synthesis of **17**, see Guana, P.; Kim, H. O.; Lee, H. W.; Tosh, D. K.; Ryu, J.-S.; Choi, S.; Jeong, L. S. Stereoselective functionalization of the 1′-position of 4′-thionucleosides. *Org. Lett.* **2006**, *19*, 4267–4270.

(13) Dong, S.; Paquette, L. A. Stereoselective synthesis of conformationally constrained 2′-deoxy-4′-thia-β-anomeric spirocyclic nucleosides featuring either hydroxyl configuration at C5′. *J. Org. Chem.* **2006**, *70*, 1580–1596.

(14) When the glycosidation was carried out utilizing **28** as a glycosyl donor, the target glycosidated product was obtained in lower yield because an unstable side product was formed. On the basis of the data of ^{1}H NMR spectrum, we assume that electrophilic addition to the ethynyl group at the 4-position of **28** would occur to lead to the side product.

(15) A similar regiochemical outcome was observed in PhSeCl-initiated electrophilic glycosidation between 3,5-*O*-(di-*tert*-butylsilylene)-4-thiofuranoid glycal and N^6-benzoyladenine; see ref 7.

(16) For detailed experimental data, see the Supporting Information.

(17) Zou, R.; Robins, M. J. High-yield regioselective synthesis of 9-glycosyl guanine nucleosides and analogues via coupling with 2-*N*-acetyl-6-*O*-diphenylcarbamoylguanine. *Can. J. Chem.* **1987**, *65*, 1436–1437.

(18) Baba, M.; DeClercq, E.; Tanaka, H.; Ubasawa, M.; Takashima, H.; Sekiya, K.; Nitta, I.; Umezu, K.; Nakashima, H.; Mori, S.; Shigeta, S.; Walker, R. T.; Miyasaka, T. Potent and selective inhibition of human immunodeficiency virus type 1 (HIV-1) by 5-ethyl-6-phenylthiouracil derivatives through their interaction with the HIV-1 reverse transcriptase. *Proc. Natl. Acad. Sci. U.S.A.* **1991**, *88*, 2356–2360.

(19) Pauwels, R.; Balzarini, J.; Baba, M.; Snoeck, R.; Schols, D.; Herdewijn, P.; Desmyster, J.; De Clercq, E. Rapid and automated tetrazolium-based colorimetric assay for the detection of anti-HIV compounds. *J. Virol. Methods* **1988**, *20*, 309–312.

(20) Ohrui, H.; Kohgo, S.; Kitano, K.; Sakata, S.; Kodama, E.; Yoshimura, K.; Matsuoka, M.; Shigeta, S; Mitsuya, S. Synthesis of 4′-*C*-ethynyl-β-D-*arabino*- and 4′-*C*-ethynyl-2′-deoxy-β-D-*ribo*-pentofuranosylpyrimidines and -purines and evaluation of their anti-HIV activity. *J. Med. Chem.* **2000**, *43*, 4516–4525.

(21) Kodama, E.; Kohgo, S.; Kitano, K.; Machida, K.; Gatanaga, H.; Shigeta, S.; Matsuoka, M.; Ohrui, H.; Mitsuya, H. 4′-Ethynyl nucleoside analogs: Potent inhibitors of multidrug-resistant human immunodeficiency virus variants in vitro. *Antimicrob. Agents Chemother.* **2001**, *45*, 1539–1546.

(22) For antiviral and cytostatic assays, see the Supporting Information.

Antivir Chem Chemother. 2011 Aug 23;22(1):51-5.

Potent anti-HIV-1 activity of N-HR-derived peptides including a deep pocket-forming region without antagonistic effects on T-20.

Izumi K, Watanabe K, Oishi S, Fujii N, Matsuoka M, Sarafianos SG, Kodama EN.

Source

Laboratory of Virus Control, Institute for Virus Research, Department of Bioorganic Medical Chemistry, Graduate School of Pharmaceutical Sciences, Kyoto University, Kyoto, Japan.

Abstract

BACKGROUND:

Enfuvirtide (T-20), a C-terminal heptad repeat (C-HR)-derived peptide of HIV-1 glycoprotein, gp41, effectively suppresses HIV-1 replication through a putative mechanism that involves it acting as a decoy and binding to the N-terminal heptad repeat (N-HR) of the virus. In this study, we address whether the anti-HIV-1 activity of T-20 is antagonized by a variety of N-HR-derived peptides.

METHODS:

Multinuclear activation of galactosidase indicator assays were used to evaluate T-20 activity in the presence of N-HR-derived peptides. The gp41-derived peptides were chemically synthesized.

RESULTS:

We demonstrate additive anti-HIV activity when T-20 is used in combination with N-HR-derived peptides that do not have a putative binding region for the tryptophan-rich domain in T-20. The presence of a deep pocket-forming region in the N-HR-derived peptides enhanced their anti-HIV-1 activity, but had little effect on the activity of T-20.

CONCLUSIONS:

These results indicate that T-20-based antiviral therapies can be combined with N-HR-derived peptides.

PMID:
21860071
[PubMed - indexed for MEDLINE]

blood

2012 119: 434-444
Prepublished online November 28, 2011;
doi:10.1182/blood-2011-05-357459

HTLV-1 bZIP factor impairs cell-mediated immunity by suppressing production of Th1 cytokines

Kenji Sugata, Yorifumi Satou, Jun-ichirou Yasunaga, Hideki Hara, Kouichi Ohshima, Atae Utsunomiya, Masao Mitsuyama and Masao Matsuoka

Blood (print ISSN 0006-4971, online ISSN 1528-0020), is published weekly by the American Society of Hematology, 2021 L St, NW, Suite 900, Washington DC 20036.

HTLV-1 bZIP factor impairs cell-mediated immunity by suppressing production of Th1 cytokines

Kenji Sugata,[1] Yorifumi Satou,[1] Jun-ichirou Yasunaga,[1] Hideki Hara,[2] Kouichi Ohshima,[3] Atae Utsunomiya,[4] Masao Mitsuyama,[2] and Masao Matsuoka[1]

[1]Laboratory of Virus Control, Institute for Virus Research, Kyoto University, Kyoto, Japan; [2]Department of Microbiology, Kyoto University Graduate School of Medicine, Kyoto, Japan; [3]Department of Pathology, School of Medicine, Kurume University, 67 Asahimachi, Kurume, Fukuoka, Japan; [4]Department of Hematology, Imamura Bun-in Hospital, Kagoshima, Japan

Adult T-cell leukemia (ATL) patients and human T-cell leukemia virus-1 (HTLV-1) infected individuals succumb to opportunistic infections. Cell mediated immunity is impaired, yet the mechanism of this impairment has remained elusive. The *HTLV-1 basic leucine zipper factor* (*HBZ*) gene is encoded in the minus strand of the viral DNA and is constitutively expressed in infected cells and ATL cells. To test the hypothesis that HBZ contributes to HTLV-1–associated immunodeficiency, we challenged transgenic mice that express the *HBZ* gene in CD4 T cells (HBZ-Tg mice) with herpes simplex virus type 2 or *Listeria monocytogenes*, and evaluated cellular immunity to these pathogens. HBZ-Tg mice were more vulnerable to both infections than non-Tg mice. The acquired immune response phase was specifically suppressed, indicating that cellular immunity was impaired in HBZ-Tg mice. In particular, production of IFN-γ by CD4 T cells was suppressed in HBZ-Tg mice. HBZ suppressed transcription from the *IFN-γ* gene promoter in a CD4 T cell–intrinsic manner by inhibiting nuclear factor of activated T cells and the activator protein 1 signaling pathway. This study shows that HBZ inhibits CD4 T-cell responses by directly interfering with the host cell-signaling pathway, resulting in impaired cell-mediated immunity in vivo. (*Blood*. 2012;119(2):434-444)

Introduction

Human T-cell leukemia virus type 1 (HTLV-1) is a retrovirus that mainly infects CD4 T cells,[1] a critical cell population for the host defense against foreign pathogens. HTLV-1 is known as the causal agent of adult T-cell leukemia (ATL),[2-4] a leukemia derived from CD4 T cells, and chronic inflammatory diseases, including HTLV-1-associated myelopathy/tropical spastic paraparesis,[5,6] alveolitis,[7] and uveitis. It has also been recognized that HTLV-1 infection is complicated by opportunistic infections caused by *Pneumocystis jiroveci*, herpes zoster virus, cytomegalovirus, or *Strongyloides stercoralis*.[8] However, the mechanism by which HTLV-1 causes immune deficiency has remained unknown.

Another human pathogenic retrovirus, HIV, replicates vigorously in vivo and produces a large number of virions. As a result of abundant viral production, HIV-infected CD4 T cells proceed to apoptosis, a phenomenon that eventually results in AIDS. In contrast, HTLV-1 increases its copy number primarily in the form of a provirus, by promoting the clonal proliferation of infected host CD4 T cells.[9,10] Despite this opposite effect on CD4 T-cell homeostasis compared with HIV, HTLV-1 infection and ATL are frequently accompanied by a deficiency of cellular immunity resembling that seen with AIDS.

HTLV-1 encodes several regulatory and accessory genes in the viral genome.[1,11] The viral proteins expressed by the integrated provirus control viral gene transcription and induce host cell proliferation, enabling HTLV-1 to achieve persistent infection. Among the viral genes of HTLV-1, *HTLV-1 bZIP factor* (*HBZ*), which is encoded in the minus strand,[12] is a constitutively expressed viral gene.[13] It has been reported that there are 2 major transcripts of the *HBZ* gene: spliced HBZ (sHBZ) and unspliced HBZ (usHBZ).[14] Based on the findings that sHBZ is more abundantly expressed than usHBZ[15] and that sHBZ has a functionally stronger effect than usHBZ,[16] we focused on sHBZ in this study.

Recently, we have reported that sHBZ expression increases the number of regulatory T cells (Tregs) by inducing transcription of the *Foxp3* gene in transgenic mice that express the *HBZ* gene in CD4 T cells (HBZ-Tg mice).[17] An increase in Tregs might be implicated in the immunodeficiency observed in ATL patients. Furthermore, previous studies have reported that HBZ suppresses host cell-signaling pathways that are critical for T-cell receptor signaling in the immune response, such as the NF-κB[18] and AP-1 pathways.[19] These findings led us to hypothesize that HBZ might have important roles in the dysregulation of cellular immunity associated with HTLV-1 infection.

To verify this hypothesis, we used HBZ-Tg mice that express sHBZ in CD4 T cells and studied well-established infection models of 2 pathogens. The first model involves intravaginal viral infection with herpes simplex virus type-2 (HSV-2). IFN-γ production by CD4 T cells is critical for the exclusion of HSV-2 from the host.[20,21] The other model involves infection with the Gram-positive intracellular bacterium, *Listeria monocytogenes* (LM), which is known as an opportunistic pathogen. In LM infection, CD4 T cells play pivotal roles in the acquired immune response by producing IFN-γ and inducing the activation of macrophages, which eliminate LM

Submitted May 27, 2011; accepted November 13, 2011. Prepublished online as Blood First Edition paper, November 28, 2011; DOI 10.1182/blood-2011-05-357459.

The online version of this article contains a data supplement.

The publication costs of this article were defrayed in part by page charge payment. Therefore, and solely to indicate this fact, this article is hereby marked "advertisement" in accordance with 18 USC section 1734.

by phagocytosis and subsequent bactericidal activity.[22,23] Indeed, previous reports have shown that some ATL patients are infected with these 2 pathogens.[24,25] Using these 2 infection models, we demonstrated that sHBZ suppresses cell-mediated immunity. Furthermore, we determined the molecular mechanism of this HBZ-mediated immune suppression.

Methods

Mice

Wild-type C57BL/6J mice were purchased from CREA Japan. Transgenic mice expressing the *sHBZ* gene under control of the CD4 promoter/enhancer/silencer have been described previously.[13] All HBZ-Tg mice were heterozygotes for the transgene. All mice used in this study were maintained in a specific pathogen-free facility and handled according to protocols approved by Kyoto University.

Herpes simplex virus type 2 infection

The HSV-2 wild-type strain UW268 and thymidine kinase (TK)-negative strain UWTK (a gift from T. Suzutani, Fukushima Medical University) used in this study were propagated and titrated on Vero cells.[26] Acyclovir was used for propagation of UWTK to block emergence of TK^+ revertant. To increase their susceptibility to HSV-2, we injected mice subcutaneously with medroxyprogesterone acetate, Depo-provera (Sigma-Aldrich), (2 mg/mouse). Five days after this hormone injection, mice were anesthetized using Avertin (Sigma-Aldrich), preswabbed with a type 2 Calgiswab (Puritan), and inoculated intravaginally with 10^3 or 10^4 plaque-forming units (PFU) of UW268. For studies of secondary infection, mice were first immunized intravaginally with 10^6 PFU of UWTK, and 4 weeks later, they were inoculated intravaginally with 10^5 PFU of UW268. Vaginal secretions were collected by 3 pipettings with 15 μL of PBS, swabbed with a Calgiswab, and added to 955 μL of 5% FCS-DMEM and stored at −80°C. HSV-2 titers were determined by plaque assay on Vero cells. Five days after primary infection, lavage fluid from the vaginal tract was harvested similarly by 3 pipettings with 20 μL of PBS.

At 6 days after infection, the vaginal tissues of infected mice were fixed in 10% formalin in phosphate buffer and embedded in paraffin. H&E staining was performed according to standard procedures. The presence of HSV-2 antigen in tissues was detected using rabbit polyclonal anti–herpes simplex virus type 2 (Dako North America). Images were captured using a Provis AX80 microscope (Olympus) equipped with OLYMPUS DP70 digital camera, and detected using a DP manager system (Olympus; original total magnification ×200).

Splenic CD4 T cells from HSV-2 primary-infected mice were stimulated in a 96-well plate coated with CD3 mAb (1 μg/mL) and CD28 mAb (1 μg/mL) for 24 hours. For antigen specific stimulation, CD4 T cells were cocultured for 48 hours in the presence of irradiated T cell–depleted splenocytes as antigen-presenting cell (APC) and heat-inactivated HSV-2 (heat inactivated at 56°C for 2 hours) at a multiplicity of infection of 1. Supernatant was collected and stored at −20°C until assay.

Evaluation of resistance and immune response to LM in mice

Wild-type LM strain EGD was used in this study. The bacterial suspension was prepared as described previously.[27] For primary infection, mice were inoculated intravenously with 10^3 colony-forming units (CFUs) of LM and the bacterial burden in the spleen was determined on day 2 or 5 after infection.

For studies of secondary infection, mice were immunized intravenously with 10^3 CFUs of LM. From day 3 through day 6.5 after immunization, the drinking water supplemented with ampicillin (2 mg/mL) was given to clear any remaining LM. On day 7, mice were challenged with 10^6 CFUs of LM, and the spleens and sera were harvested after 3 or 12 hours. Spleens were homogenized in PBS, and the number of viable bacteria was determined by plating 10-fold serial dilutions on tryptic soy agar plates and counting the CFUs.

For cytometric assays, immunized mice were re-inoculated with 10^7 CFUs of LM. Splenocytes were harvested after 12 hours, cultured in the presence of protein transport inhibitor for 6 hours, and evaluated by the FACSCanto II (BD Biosciences) for cell surface and intracellular markers.

To determine the functional development of CD4 T cells in immunized mice, we purified splenic CD4 T cells and then stimulated them in a 96-well plate coated with CD3 mAb and CD28 mAb. For LM specific stimulation, CD4 T cells were cocultured with mouse bone marrow–derived macrophages (BMDMs) differentiated in the presence of 100 ng/mL of M-CSF and pulsed with viable LM at a multiplicity of infection of 10. Supernatant after stimulation for 24 hours was collected and stored at −20°C until assay.

Analysis of virus vector-transduced CD4 T cells

Retroviral transduction was performed as described previously.[17] The spliced HBZ gene was cloned into a retroviral vector, pMXs-Ig (a gift from T. Kitamura, The University of Tokyo), to generate pMXs-Ig-HBZ. This plasmid DNA was transfected into the packaging cell line, Plat-E. For retroviral transduction, $CD25^-CD4^+$ cells were enriched by a CD4 enrichment kit (BD Biosciences PharMingen) and were activated by anti-CD3 Ab (0.5 μg/mL) and rIL-2 (50 U/mL) in the presence of T cell–depleted and x-irradiated (20 Gy) C57BL/6J splenocytes as APCs in 12-well plates. After 16 hours, activated T cells were transduced with viral supernatant in the presence of 4 μg/mL polybrene and centrifuged at 1700*g* for 60 minutes. Then, transduced CD4 T cells were stimulated by phorbol 12-myristate 13-acetate (PMA; 50 ng/mL) and ionomycin (1 μg/mL) or plate-coated CD3 mAb (1 μg/mL) and CD28 mAb (1 μg/mL) in the presence of protein transport inhibitor and analyzed by a flow cytometry as shown in Figure 3. Dead cells were excluded using forward and side scatter and LIVE/DEAD Fixable Dead Cell Stain Kit (Invitrogen) by flow cytometry. Thereafter, intracellular cytokines were measured.

For generation of the lentivirus vector, sHBZ cDNA was cloned into pCS2-EF-GFP (a gift from H. Miyoshi, RIKEN BioResource Center) as previously described.[13] In brief, 293FT cells were cotransfected with the lentivirus vector, pCMV-Δ8/9 and pVSVG and supernatant containing virus was used for transduction. The lentivirus titer was determined on 293FT cells.

Empty vectors that express only GFP were used as controls for retroviral and lentiviral transductions.

IFN-γ promoter assay

Nucleotides −670 to +64 of the IFN-γ promoter region were amplified by PCR using human genomic DNA as a template, and cloned into pGL4.22 (Promega). The PathDetect pAP-1-Luc and pNFAT-Luc Cis-Reporter Plasmids were purchased from Promega. Transfection and luciferase assay were performed according to supplemental Methods (available on the *Blood* Web site; see the Supplemental Materials link at the top of the online article).

ChIP assay

sHBZ-expressing Jurkat cells were stimulated with PMA and ionomycin. ChIP assay was performed as reported previously.[28] ChIP DNA samples were subjected to the StepOnePlus real-time PCR system using Power SYBR Green PCR Master Mix (Applied Biosystems). The sequences of the primers for the human IFN-γ promoter were: 5′-TACCAGGGC-GAAGTGGGGAG-3′ (sense) and 5′-GGTTTTGTGGCATTTGGGTG-3′ (anti-sense).

Statistical analysis

For in vitro and in vivo experiments, multiple data comparisons were performed using the Student unpaired *t* test.

Results

High susceptibility of HBZ-Tg mice to HSV-2 infection

We first evaluated the susceptibility of HBZ-Tg mice to HSV-2 infection. Recently, we reported that HBZ-Tg mice frequently develop T-cell lymphoma and dermatitis after 10 weeks.[17] Therefore, HBZ-Tg mice without skin symptoms at 7 to 10 weeks of age were used in this study. It has been reported that the host immune response against primary HSV-2 infection can be divided into 2 stages: the innate immune response plays a dominant role by day 2 after infection, whereas cellular immunity plays an important role later, after day 5 after infection.[29] IFN-γ production by CD4 T cells is known as a critical factor in the cellular immune response against pathogens.[29] To determine whether cellular immunity is impaired in HBZ-Tg mice, we pretreated HBZ-Tg and non-Tg mice with Depo-provera for efficient infection and inoculated them with HSV-2 through the vaginal route.[30] The viral titer of HSV-2 in the lesion was measured. In this primary infection assay, there was no significant difference in the viral titers between non-Tg and HBZ-Tg mice at day 2 after inoculation (Figure 1A), when innate immunity is responsible for the host defense. In contrast, at day 6 after infection, when acquired immunity becomes important, HBZ-Tg mice showed significantly higher viral titers of HSV-2 than non-Tg mice (Figure 1A). Immunohistochemical analysis revealed that abundant viral antigens were detected in the vaginal epithelial cells and ganglia of HSV-2 challenged HBZ-Tg mice but not in non-Tg mice (Figure 1B).

To explore the mechanism of this immune deficiency, we examined cytokine production by CD4 T cells stimulated with antibodies to CD3 and CD28 or with heat-inactivated HSV-2 and APC. On day 6 after infection, the production of Th1 effector cytokines, including IFN-γ, IL-2, and TNF-α, was significantly reduced in CD4 T cells from HBZ-Tg mice compared with non-Tg mice (Figure 1C). Furthermore, IFN-γ concentration in vaginal wash fluids at day 5 after infection was significantly suppressed in HBZ-Tg compared with non-Tg mice (Figure 1D). When we challenged mice with a 50% lethal dose of HSV-2, the survival rate of non-Tg mice at day 20 after infection was 53%. In contrast, HBZ-Tg mice could not survive a viral challenge at the same dose (Figure 1E).

To study acquired immunity against HSV-2, we immunized and challenged mice as shown in Figure 1F. First, mice were immunized by TK-negative HSV-2 strain, the attenuated mutant of HSV-2, and then they were challenged with wild-type HSV-2. The vaginal virus titer in HBZ-Tg mice at day 3 after challenge was similar to that in nonimmune non-Tg mice (Figure 1F), whereas HSV-2 was not detected in immune non-Tg mice. The difference in viral titer between non-Tg and HBZ-Tg mice was much more remarkable in these secondary infection experiments than in the previous primary infection experiments, implicating impaired acquired immunity in HBZ-Tg mice. These results demonstrate that expression of sHBZ in CD4 T cells induces a deficiency in the immune response against HSV-2 and impairs the production of IFN-γ, IL-2, and TNF-α.

HBZ-Tg mice have an impaired T cell–dependent immune response to LM

We next evaluated the susceptibility of HBZ-Tg mice to infection with LM via an intravenous route. As with HSV-2 infection, production of IFN-γ by CD4 T cells plays a crucial role in the growth inhibition and elimination of LM in vivo.[31,32] On day 2 or 5 after primary infection with LM, we removed spleens and evaluated the bacterial burdens in the organs. The number of LM recovered from HBZ-Tg spleen on day 2 was comparable to that from non-Tg mice, yet the bacterial burden in HBZ-Tg mice at day 5 was higher than that in non-Tg mice (Figure 2A), suggesting a reduced protection in HBZ-Tg mice against LM, especially when acquired immunity is being established. We next a performed secondary infection experiment to evaluate the T cell–dependent immunity that developed after primary infection. Non-Tg mice immunized with a small dose of LM and later challenged with a high dose exhibited a significant level of bacterial elimination 12 hours after challenge compared with nonimmunized mice (Figure 2B). By contrast, such a significant level of bacterial elimination was not observed in immunized HBZ-Tg mice (Figure 2B), indicating that acquired LM-specific immunity is impaired in HBZ-Tg mice.

Characterization of cytokine production in the LM-infected mice

We next measured the concentration of several cytokines in the sera and homogenized spleen supernatant of HBZ-Tg and non-Tg mice during secondary infection with LM. IFN-γ, TNF-α, IL-2, IL-6, and IL-10 were decreased in HBZ-Tg mice (Figure 2C) compared with non-Tg mice. On the other hand, IL-12, which is mainly secreted by APCs, was increased in HBZ-Tg at 12 hours. To explore whether impaired production of Th1 cytokines by CD4 T cells is responsible for the decrease in levels of IFN-γ, TNF-α, and IL-2 in the serum, we enriched CD4 T cells from the spleens of immunized mice and then stimulated the cells ex vivo nonspecifically (with mAbs to CD3 and CD28) or specifically (with BMDMs pulsed with viable LM). The ability of CD4 T cells from HBZ-Tg mice to produce IFN-γ and IL-2 in response to either kind of stimulation was markedly impaired compared with that of cells from non-Tg mice (Figure 2D). In contrast, a considerable amount of TNF-α production was detected in tests of both HBZ-Tg and non-Tg CD4 T cells after stimulation with LM-pulsed BMDMs. However, this level of TNF-α was almost comparable with that observed in the culture of LM-pulsed BMDMs alone (Figure 2D). Therefore, the TNF-α detected in this experiment was probably produced by the macrophages, not by the CD4 T cells. These results strongly suggest that the ability of CD4 T cells to produce Th1 cytokines is impaired in HBZ-Tg mice.

Because IFN-γ is reported to play a pivotal role in the acquired protection of mice against LM,[22,23] we focused on IFN-γ production by LM-specific CD4 T cells. Splenic cell suspensions were prepared from 2 groups of mice immunized and challenged according to the protocol shown in Figure 2B. Cells were cultured for 6 hours in the presence of protein transport inhibitor and then subjected to flow cytometric analysis for IFN-γ production by intracellular cytokine staining. The number of IFN-γ–producing CD4 T cells in HBZ-Tg mice was remarkably reduced compared with that in non-Tg mice (Figure 3A). In contrast, IFN-γ production by CD8 T cells showed no significant difference between non-Tg and HBZ-Tg mice (Figure 3A). In addition, there were no differences between HBZ-Tg mice and control littermates in both total and $CD4^+$ splenocytes (supplemental Figure 1).

We recently reported that the proportion of $Foxp3^+$ $CD4^+$ T cells is increased in HBZ-Tg mice.[17] A previous study reported that Foxp3 expression inhibits the production of IFN-γ,[33] suggesting that a decreased proportion of effector T cells in HBZ-Tg mice might be responsible for the low number of IFN-γ–producing CD4

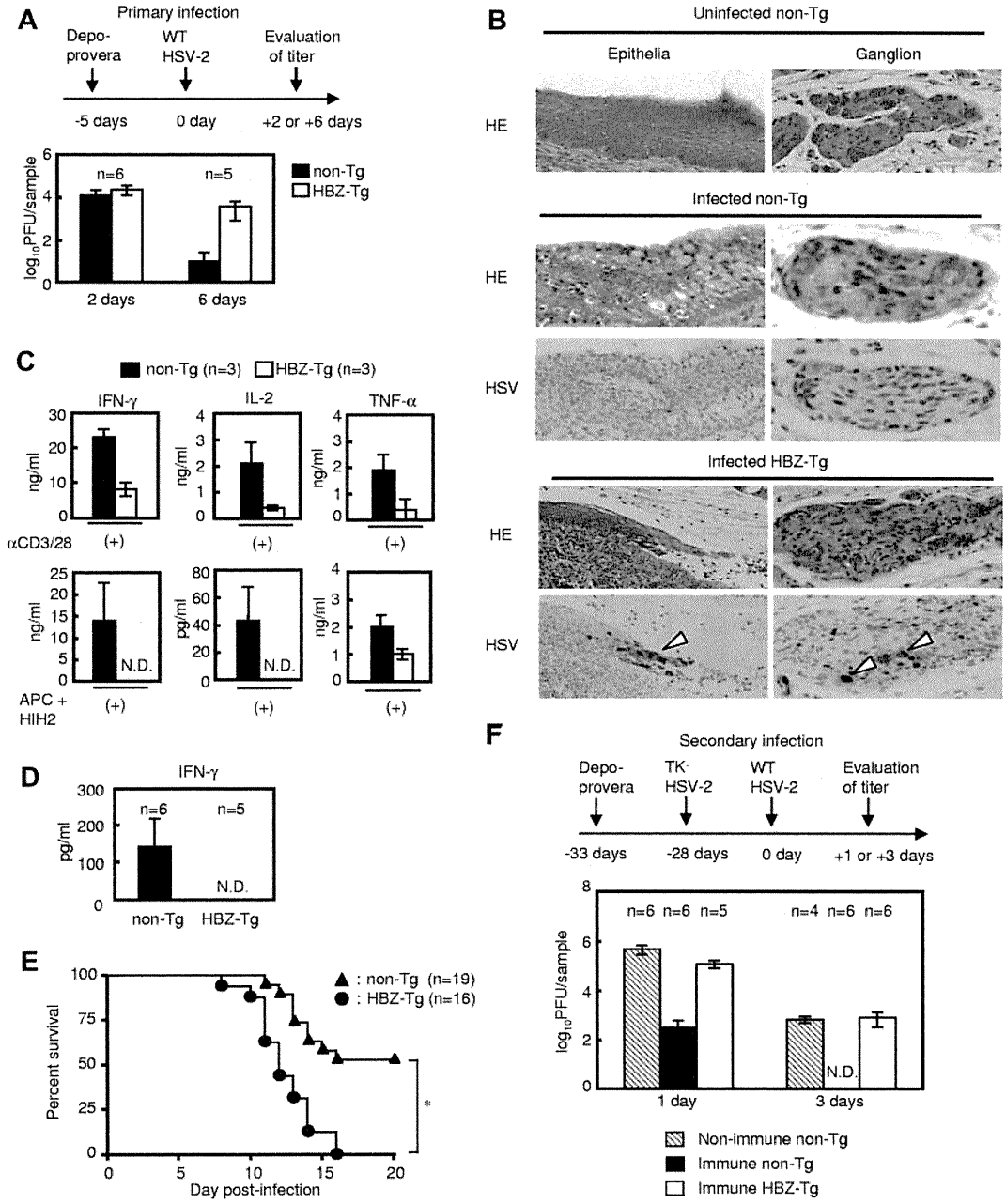

Figure 1. Transgenic mice expressing sHBZ in CD4 T cells are highly susceptible to intravaginal infection with HSV-2. (A) Virus titer in vaginal washes in primary infection. (B) Histologic analysis of epithelia and ganglion in vaginal tissue from mice infected with HSV-2. Uninfected vaginal tissues are presented as controls. HE indicates H&E stain; and HSV, immunohistochemical analysis for the viral antigen. Arrowheads indicate HSV-2–positive cells. (C) Cytokine production by splenic CD4 T cells from mice infected with 10^4 plaque-forming units (PFU) of HSV-2. Cells were stimulated with mAbs to CD3 and CD28 or APC plus heat-inactivated HSV-2 (HIH2) in ex vivo culture. (D) IFN-γ concentration in vaginal wash fluid harvested at day 5 after infection. (E) Survival curve of non-Tg or HBZ-Tg mice infected with 10^3 PFU of HSV-2. *$P < .05$ (log-rank test). (F) Viral titer in vaginal washes during HSV-2 secondary infection. To evaluate adaptive immunity against HSV-2 infection, mice were immunized and infected with the virus as shown in the upper panel. Bars represent the mean ± SD of all mice per genotype. Two or 3 independent experiments have been performed. N.D. indicates not detected.

T cells. However, the impairment of IFN-γ production was still observed in the Foxp3-negative effector CD4 T-cell population (Figure 3B), indicating that the reduction in IFN-γ production is independent of Foxp3 expression. These results collectively indicate that transgenic expression of sHBZ in CD4 T cells results in a reduction in effector cytokine production by CD4 T cells.

sHBZ directly inhibits IFN-γ production in a CD4 T cell–intrinsic manner

To determine whether sHBZ-mediated IFN-γ suppression was induced by a cell-intrinsic effect of sHBZ in CD4 T cells or by a dysregulated immunologic status in vivo indirectly caused by sHBZ expression, we used a retrovirus vector to express sHBZ in naive CD4 T cells. Wild-type CD4 T cells transduced with sHBZ showed lower IFN-γ production than empty vector-transduced cells (Figure 4A-B), demonstrating that sHBZ directly suppresses IFN-γ production in CD4 T cells. It is noteworthy that sHBZ suppressed IFN-γ production in human CD4 T cells as well as mouse T cells. This suppression was not limited to IFN-γ but was also observed for TNF-α (Figure 4C) and IL-2 (Figure 4D). Expression level of the *HBZ* gene transcript was much higher than that of HBZ-Tg mice (supplemental Figure 2). IL-4 production was

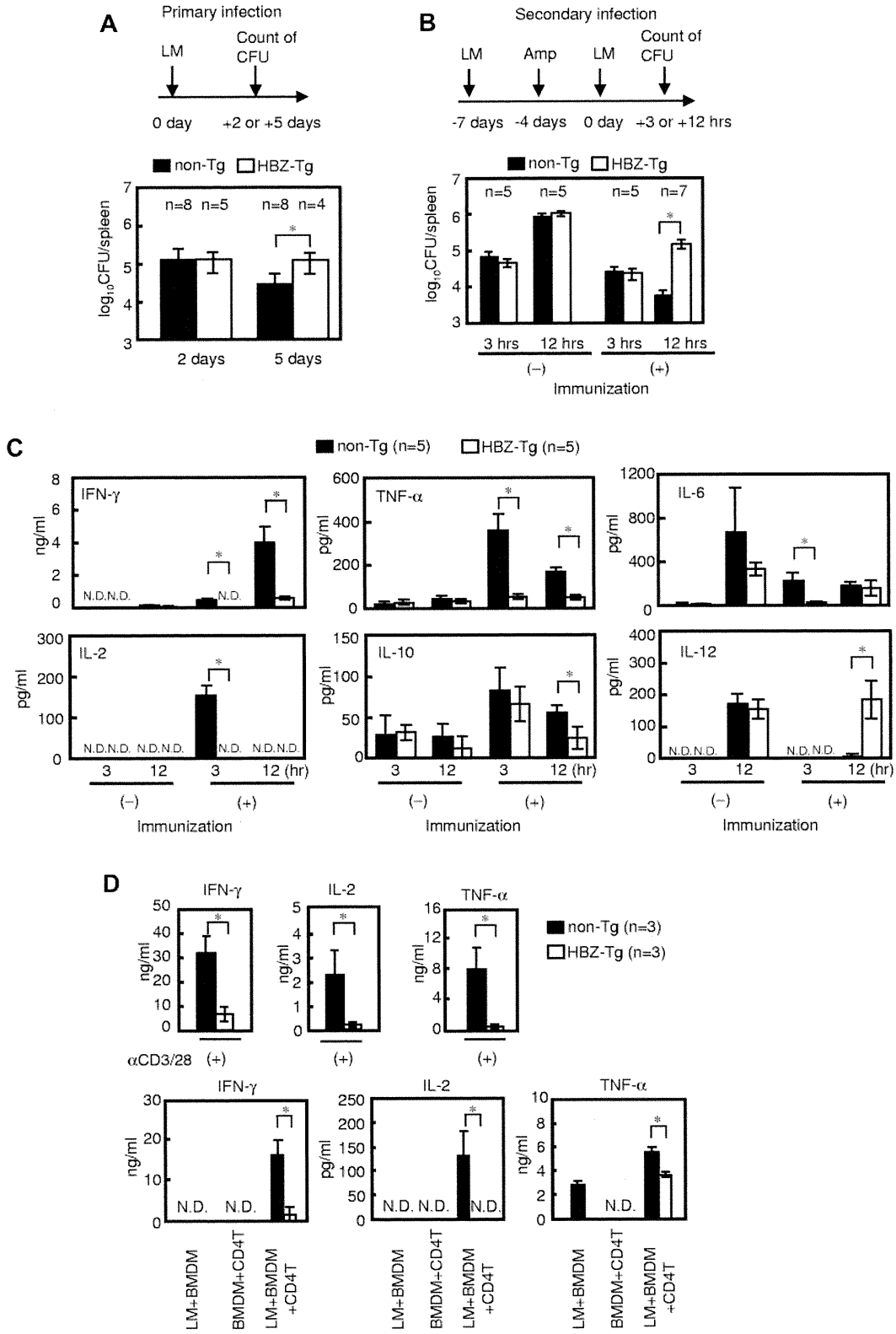

Figure 2. HBZ-Tg mice show decreased immune response to primary and secondary infection with LM. Bacterial loads of spleens from mice challenged with LM in primary (A) and secondary (B) infection are shown. (C) Concentrations of IFN-γ, TNF-α, IL-2, IL-6, and IL-12 in serum and IL-10 in homogenized spleen supernatant from the secondarily infected mice. (D) Cytokine production by CD4 T cells from secondarily infected mice. Mice were immunized as shown in panel B. CD4 T cells were stimulated ex vivo with mAbs to CD3 and CD28 or with LM-infected WT-BMDMs. Bars represent the mean ± SD of all mice per genotype. Two independent experiments have been performed; representative results are shown. *$P < .05$ by Student t test. N.D. indicates not detected.

not detected in CD4 T cells (supplemental Figure 3A). Although production of Th1 cytokines was reduced in sHBZ-expressing CD4 T cells, IL-6 and IL-10 production was not altered by sHBZ expression (supplemental Figure 3B-C). These results collectively suggest that sHBZ expression in HTLV-1–infected CD4 T cells inhibits transcription of the *IFN-γ*, *TNF-α*, and *IL-2* genes, which

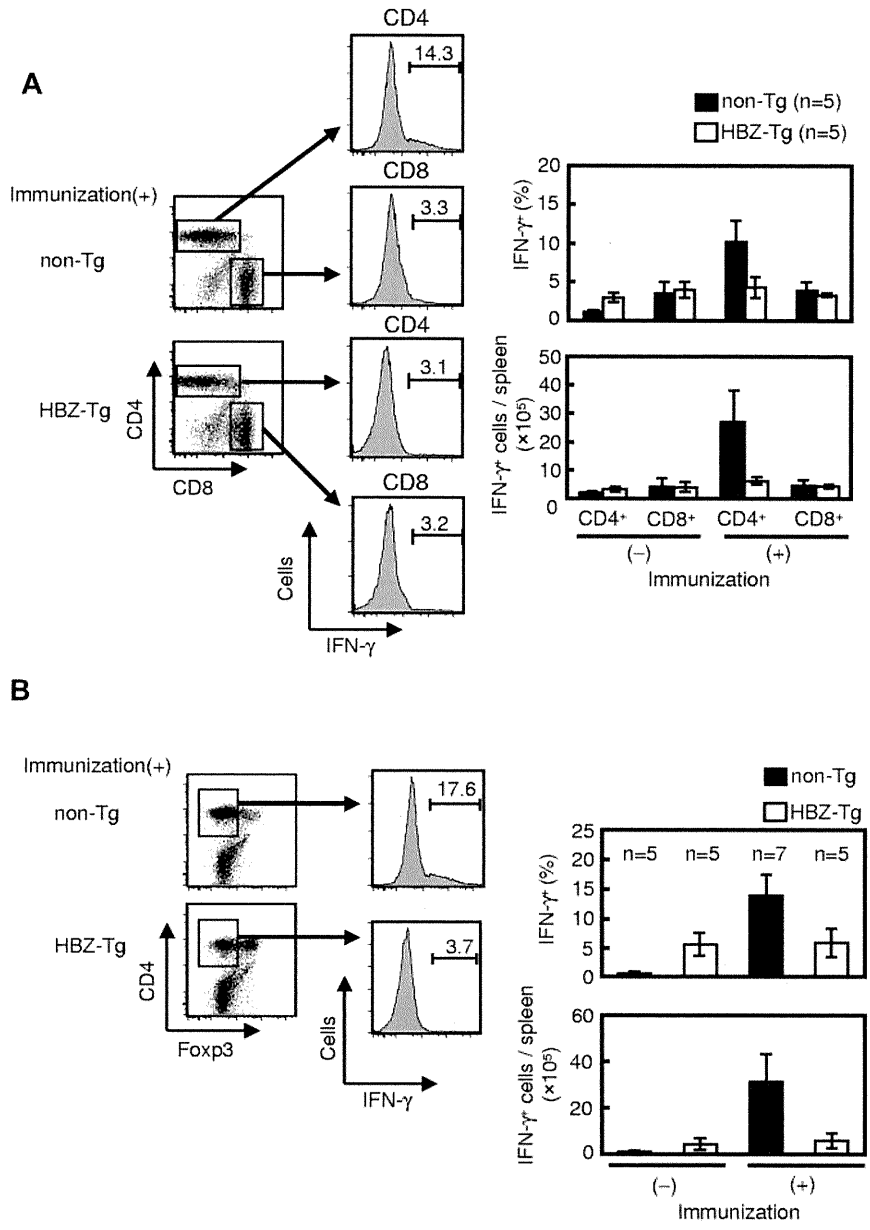

Figure 3. IFN-γ production by CD4 splenocytes from LM secondarily infected HBZ-Tg mice decreases in CD4⁺ Foxp3⁻ T cells. Mice were immunized and challenged as shown at the top of Figure 2B, and their splenocytes were harvested at 12 hours after challenge and analyzed for intracellular IFN-γ production. (A) Splenocytes were gated by CD3 expression, and IFN-γ production was measured in living CD4 or CD8 T cells using FACS. (B) IFN-γ production in CD3⁺ CD4⁺ Foxp3⁻ cells was determined. Bars represent the mean ± SD of all mice per genotype. Two independent experiments have been performed.

play important roles in the immune response against foreign pathogens.

sHBZ suppresses the activity of the IFN-γ promoter by inhibiting the NFAT and AP-1 signaling pathways

To further elucidate the mechanism of sHBZ-mediated IFN-γ inhibition, we performed a promoter assay using a human −670 to +64 IFN-γ promoter construct in the human T-cell line Jurkat. Previous reports have demonstrated that NFAT, AP-1, and NF-κB signaling pathways are involved in the regulation of *IFN*-γ transcription.[34] We found that PMA and ionomycin treatment enhanced IFN-γ promoter activity, and sHBZ suppressed this enhancement in a dose-dependent manner (Figure 5A). In contrast, another viral protein, Tax, enhanced the promoter activity as reported previously (Figure 5B),[35] an observation that is in line with previous findings that Tax is capable of activating the NF-κB and AP-1 signaling pathways.[36] Previous studies have demonstrated that the level of *sHBZ* transcripts in ATL patients and HTLV-1 carriers is approximately 4-fold higher than the level of *tax* transcripts.[15] The activation of the IFN-γ promoter by Tax was inhibited by sHBZ when sHBZ was expressed at levels similar to those in HTLV-1 carriers (Figure 5C), suggesting that sHBZ can have an inhibitory effect on Tax-mediated IFN-γ induction in HTLV-1 infected cells.

To identify the region of the IFN-γ promoter responsible for sHBZ-mediated suppression, we conducted further analyses using serially deleted promoter constructs. The human IFN-γ promoter (−670 to +64) contains NFAT, AP-1, STAT, ATF, and T-bet binding regions, and these transcription factors are reported to be involved in IFN-γ expression. The suppressive effect of sHBZ on the IFN-γ promoter was reduced by the deletion between dM2 and dM3 ($P < .001$; Figure 5D: a deletion, which removes 2 NFAT sites, an AP-1 site, and a STAT binding site). Because HBZ has a suppressive effect on the NFAT and AP-1 signaling pathways,[17,19] these binding sites might be associated with the suppressive effect of sHBZ. To further explore this possibility, we generated the promoter constructs with point mutation for each NFAT or AP-1 sites, and performed the promoter assay. The point mutation for

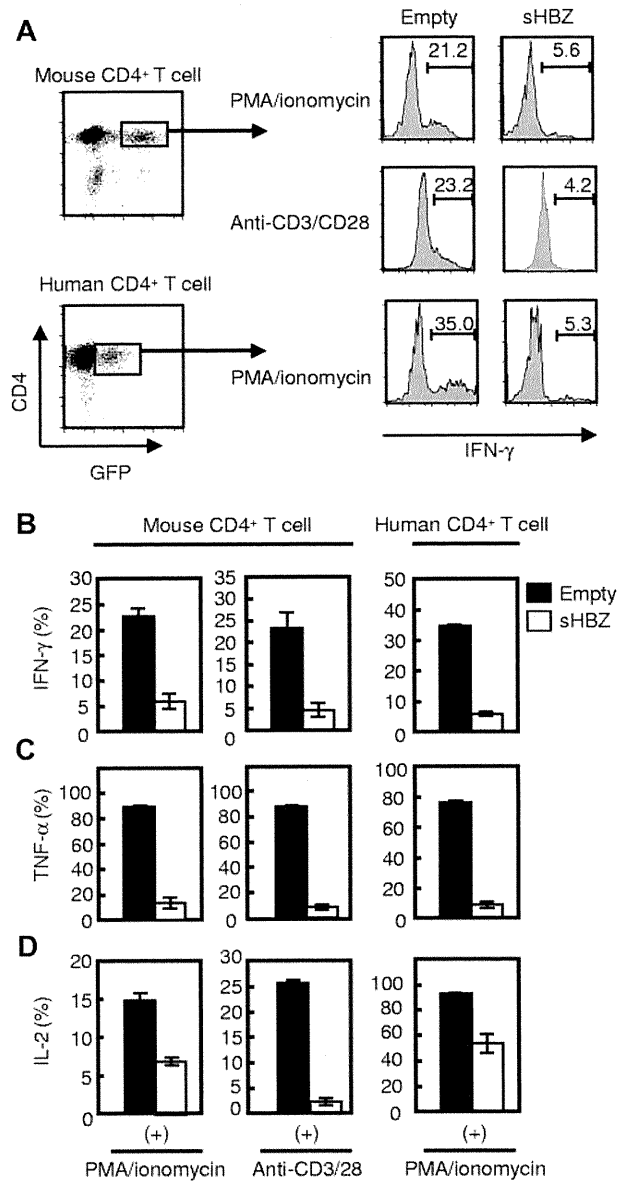

Figure 4. sHBZ directly inhibits IFN-γ production in both human and mouse CD4 T cells. Mouse and human CD4 T cells were transduced with recombinant retroviruses or lentiviruses, respectively, expressing sHBZ, and stimulated with PMA and ionomycin or antibodies to CD3 and CD28. Then, intracellular cytokines in living HBZ-expressing CD4 T cells were measured using FACS. (A) GFP$^+$ and CD4$^+$ cells were gated as shown in the left panel and evaluated for intracellular production of IFN-γ, TNF-α, or IL-2 by flow cytometry. Representative histograms of IFN-γ are shown. (B-D) Percentages of IFN-γ$^+$ (B), TNF-α$^+$ (C), or IL-2$^+$ (D) cells in mouse and human CD4 T cells. Representative data from 2 independent experiments in triplicate (mean ± SD) are shown.

−163 to −153 (P = .025) but not −279 to −269 (P = .057) NFAT binding site remarkably reduced suppressive effect of promoter activity by HBZ (Figure 5E). We next characterized effect of sHBZ on AP-1 binding sites in the IFN-γ promoter. The point mutation for −193 to −183 AP-1 binding site partially impaired the inhibitory effect (P = .042; Figure 5F). Three point mutations of all AP-1 binding sites much more reduced the HBZ-mediated suppressive effect on the promoter (P = .001; Figure 5F). These results indicate that NFAT and AP-1 binding sites are involved in the suppressive effect of HBZ on this promoter.

To further elucidate the involvement of the AP-1 or NFAT signaling pathway in the sHBZ-induced impairment of IFN-γ production, we used sHBZ mutants, which are unable to exert an inhibitory effect on NFAT or AP-1 signaling. We have reported that activation and central domains of HBZ interacted with NFAT.[17] We constructed deletion mutants and 7 amino-acid substitution mutants of sHBZ central domain and assessed their abilities to function in the NFAT or AP-1 signaling pathway (Figure 6A-B; supplemental Figure 4A-C). We found 2 mutants of interest: sHBZ-CDm7 and sHBZ-ΔAD. sHBZ-CDm7 contained amino acid substitutions in the central domain of sHBZ, and these mutations abrogated the inhibitory effect of sHBZ on the activity of an NFAT reporter plasmid (Figure 6A). In contrast, sHBZ-ΔAD, which contains a deletion of the activation domain of sHBZ, did not have suppressive activity on the AP-1 signaling pathway (Figure 6B). We confirmed that expression levels of the sHBZ mutants were comparable with that of WT-sHBZ (supplemental Figure 4D). Consistent with the findings of the reporter assay with the deleted promoters, sHBZ-CDm7 and sHBZ-ΔAD showed remarkable reduction in the inhibitory effect on the IFN-γ promoter (Figure 6C). Furthermore, we generated retrovirus vectors that express these sHBZ mutants, transduced them to mouse CD4 T cells, and evaluated their effect on IFN-γ production. We found that these 2 sHBZ mutants lost their inhibitory effect on IFN-γ production compared with WT-sHBZ (Figure 6D). Previous reports have shown that bZIP domain of HBZ plays a role in suppression for transcriptional activity of AP-1 family, including c-Jun and JunB.[19,37] In this study, deletion mutant of bZIP domain in sHBZ did not influence NFAT and AP-1 pathway in Jurkat cell (Figure 6A-B) and IFN-γ production in mouse CD4$^+$ T cell (supplemental Figure 5A), indicating that not bZIP domain but activation domain of HBZ is essential for suppression of AP-1 pathway in this study.

In addition, we performed a ChIP assay to explore recruitment of the transcription factors NFAT and AP-1 to the IFN-γ promoter in the presence of sHBZ. This experiment showed that sHBZ inhibited recruitment of NFATc2 and c-Jun to the IFN-γ promoter containing 2 NFAT sites and one AP-1 binding site (Figure 6E). These results suggest that sHBZ physically inhibits DNA binding of c-Jun and NFATc2 and suppresses the NFAT and/or AP-1 signaling pathways, which are critical for IFN-γ production in CD4 T cells.

Impaired production of IFN-γ in primary ATL cells

Jurkat T cells express *IFN-γ* gene transcripts after stimulation with PMA and ionomycin. sHBZ expression in Jurkat cells remarkably reduced the level of *IFN-γ* mRNA (Figure 7A). It is critical to study IFN-γ expression in naturally HTLV-1–infected T cells. Therefore, we examined IFN-γ production in PBMCs from ATL patients (supplemental Table 1). PBMCs were stimulated by PMA and ionomycin for 5 hours, and intracellular IFN-γ was stained. We found that IFN-γ production by CD4 T cells was remarkably decreased in ATL patients compared with healthy donors (Figure 7B). In addition, TNF-α and IL-2 production also was suppressed in CD4 T cells from ATL patients. These data suggest that impaired production of IFN-γ is observed not only in HBZ-Tg or ectopically transfected cells but also in primary CD4 T cells from ATL patients.

Discussion

Viruses that cause chronic infections, including hepatitis C virus, HIV, Epstein-Barr virus, and HTLV-1, have strategies to evade the host immune system and to replicate in vivo despite detectable immune responses.[38] For HTLV-1, it has been reported that p12 binds to free human major histocompatibility complex class

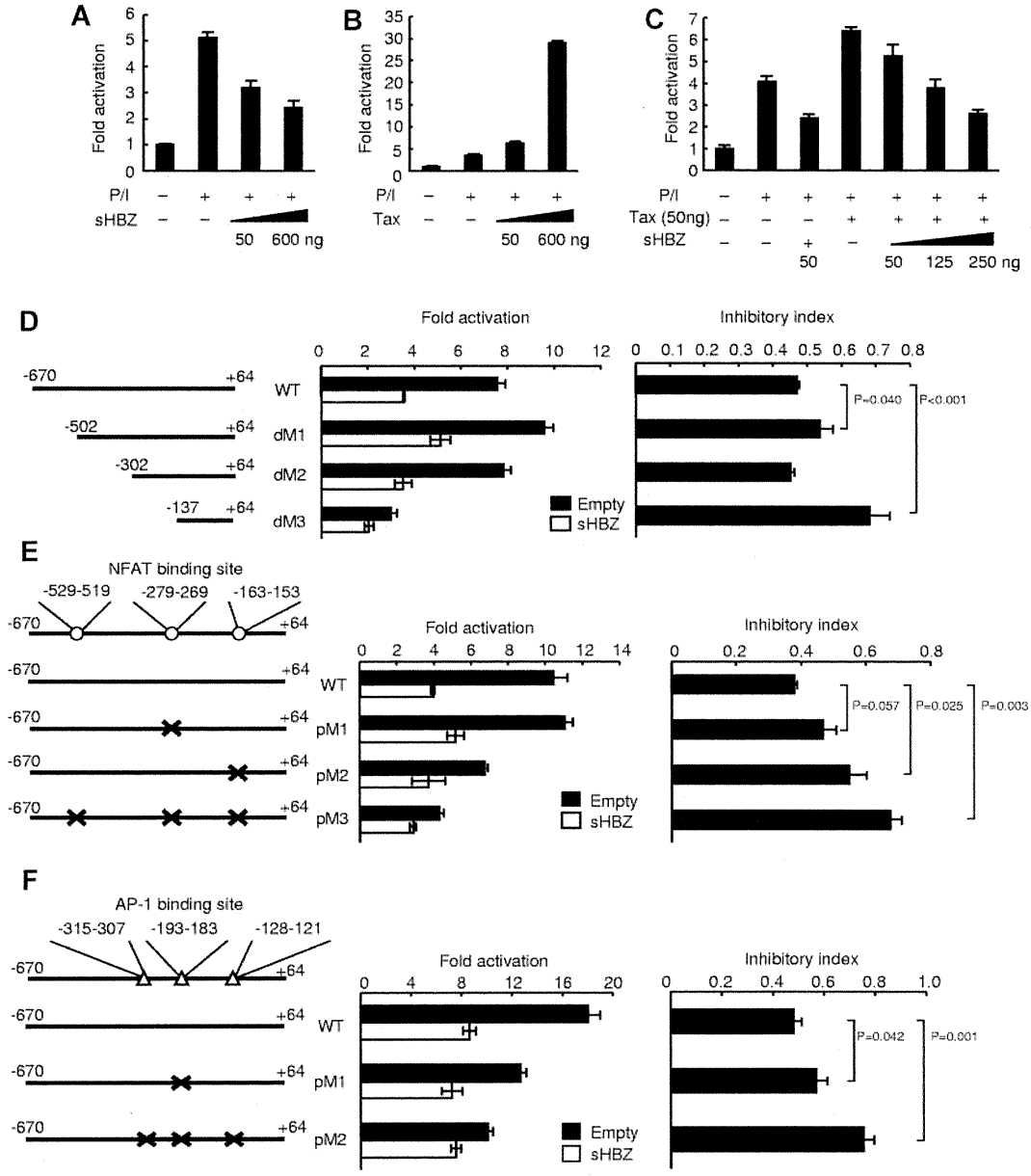

Figure 5. sHBZ suppresses IFN-γ promoter activity. Luciferase assay of the IFN-γ promoter reporter constructs (−670 to +64) cotransfected with an expression plasmid for sHBZ (A), Tax (B), or both (C) is performed in Jurkat cells, which were stimulated with PMA and ionomycin. Luciferase assays of reporter plasmids containing deletions (D) or point mutations in the NFAT (E) or AP-1 (F) consensus-binding region of IFN-γ promoter are performed. The positions of the deleted or mutated regions are indicated in the left of each graph. Consensus sequences for NFAT and AP-1 binding sites were mutated. Inhibitory index is represented as a ratio of fold activation with empty vector or HBZ expression vector. Representative data (mean ± SD) from 2 independent experiments in triplicate are shown.

I heavy chains and inhibits its expression, which results in escape of infected cells from host immune system.[39] A number of viruses evade the host immune response by perturbing the production of cytokines. It has been reported that the core protein of HCV decreases IL-2 production via suppression of mitogen-activated protein kinase.[40] The vaccinia virus double-strand RNA binding protein E3 inhibits the PKR, NF-κB, and IRF3 pathways, thus suppressing IFN-β, TNF-α, and TGF-β production.[41] The HIV-1 Tat protein perturbs signal transduction by IFN-γ.[42] However, it has not been known precisely how HTLV-1 evades the host immune system. In this study, we show that sHBZ inhibits the effector function of CD4 T cells via interaction with NFAT and AP-1, leading to a suppressive effect on the production of Th1 cytokines, such as IFN-γ. This is probably a mechanism of the cellular immune deficiency observed in HTLV-1 infection.

It is well known that NF-κB, AP-1, and NFAT are involved in T-cell receptor signaling pathways.[43] Tax is broadly recognized to play a crucial role in the pathogenesis of HTLV-1, including oncogenesis and inflammation. Previous studies showed that Tax could activate cellular signaling pathways, including NF-κB, and AP-1.[36] Thus, Tax has an enhancing effect, not a suppressive effect, on the immune response of infected cells. On the other hand, HBZ is constitutively transcribed in infected cells and suppresses cellular signaling pathways, including the CREB, AP-1, and canonical NF-κB pathways.[44] These findings suggest that HBZ, rather than Tax, is probably responsible for the immune deficiency in HTLV-1 infection and may act through the impairment of effector cytokine production. Indeed, this study shows that sHBZ suppresses the *IFN-γ* transcription through interaction with NFAT and c-Jun.

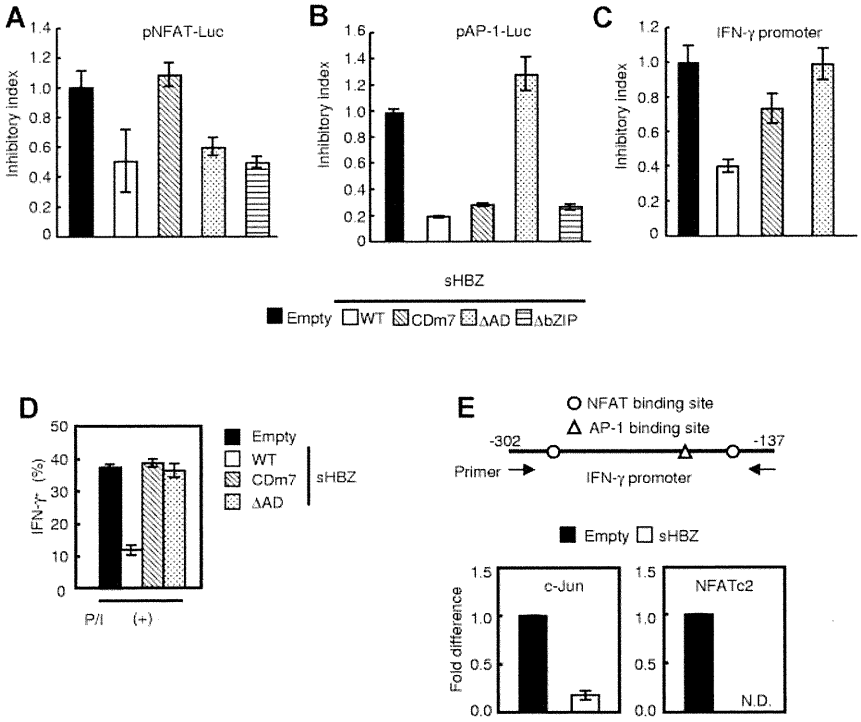

Figure 6. NFAT and AP-1 signaling pathways are responsible for HBZ-mediated inhibition of IFN-γ production. (A-C) Effects of wild-type and mutant sHBZ on (A) an NFAT-Luc reporter, (B) an AP-1-Luc reporter, and (C) the IFN-γ promoter. (D) The suppressive effect of sHBZ mutants on IFN-γ production from primary mouse CD4 T cells. Retroviruses expressing wild-type and mutated HBZ were transduced to primary mouse CD4 T cells, stimulated with PMA and ionomycin, and stained. (E) ChIP assay of the NFAT and AP-1 binding sites of IFN-γ promoter. sHBZ-expressing Jurkat cells were stimulated with PMA and ionomycin, and ChIP assay was performed using anti-NFATc2 or anti–c-Jun antibodies. The IFN-γ promoter (−302 to −137) was amplified by real-time PCR. The data from stimulated empty-transfected Jurkat cells were used as a reference. Representative data (mean ± SD) from 2 or 3 independent experiments are shown. N.D. indicates not detected.

We have recently reported that the HBZ-Tg mice used in this study harbor increased numbers of $CD4^+$ $Foxp3^+$ Tregs compared with non-Tg mice.[17] Tregs are known as negative regulators of the host immune response to pathogens[45]; hence, an increase in the number of Tregs might contribute to the suppression of effector T-cell responses against HSV-2 or LM in vivo. Tregs suppress the memory CD8 T-cell response.[46] However, we found that the production of IFN-γ was impaired in sHBZ-expressing CD4 T cells but not in CD8 T cells (Figure 3A). IFN-γ production was impaired in a CD4 T cell–intrinsic manner. In addition, the suppressive effect of Tregs on IFN-γ production by effector CD4 T cells was not observed in mice immunized with LM (supplemental Figure 6). Taken together, these data imply that the increased number of Tregs is not the main cause of the CD4 T-cell specific reduction of IFN-γ production; rather, sHBZ expression in CD4 T cells may lead directly to suppressed production of IFN-γ.

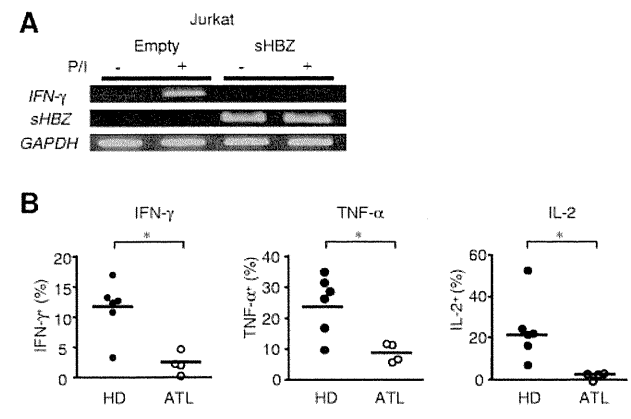

Figure 7. IFN-γ production is suppressed in sHBZ-expressing Jurkat cells and PBMCs of ATL patients. (A) sHBZ inhibits *IFN-γ* gene transcription after stimulation with PMA and ionomycin. Transcripts of the *IFN-γ* and *sHBZ* genes were analyzed by RT-PCR. (B) IFN-γ, TNF-α, and IL-2 production by CD4 T cells in PBMCs from healthy donors (HD; n = 6) and ATL patients (n = 4). PBMCs were separated from the peripheral blood and then stimulated with PMA and ionomycin for 5 hours. Thereafter, intracellular production of Th1 cytokines in living cells was measured by flow cytometry. The y-axis indicates the percentages of cytokine-producing cells in CD4 T cells. *$P < .05$ by Student *t* test.

In this study, we evaluated the cell-mediated immunity of HBZ-Tg mice against HSV-2 and LM. The protective immune response to these pathogens is mediated by IFN-γ production by NK cells, CTLs, and/or Th1 cells.[47] IFN-γ up-regulates major histocompatibility complex molecules, and inducible nitric oxide synthase, activates NK cells and macrophages, and induces Th1 development,[47] thus leading to the elimination of HSV-2 and LM. Lack of IFN-γ function (because of mutation of IFN-γ or its receptor, or because of the presence of IFN-γ specific antibody) in vivo increases susceptibility to many pathogens, including lymphocytic choriomeningitis virus, *Mycobacterium tuberculosis*, and *Leishmania major*.[47] Of particular interest is the fact that protection against infection with *Cryptosporidium parvum*,[48] or *Candida albicans*,[49] which cause opportunistic infections in immune compromised hosts, depends on IFN-γ production from CD4 T cells. In addition, previous reports have shown that a lack of CD4 T-cell help during primary infection results in an incomplete memory immune response in which CTL activity and antibody production by plasma cells are impaired.[50] Our current results, therefore, indicate that the reduced production of helper cytokine caused by sHBZ expression in CD4 T cells may contribute to the immunodeficiency observed in HTLV-1–infected persons and in HBZ-Tg mice.

Previous studies reported that activation and bZIP domains of HBZ played important roles in suppressive effects on the AP-1 pathway.[19,37] However, this study showed that only activation domain was critical in T cells when stimulated by PMA and ionomycin. Deletion of bZIP domain partially impaired AP-1 activation by Tax (supplemental Figure 5B). Previous studies used 293T cells and stimulated them by expression of c-Jun or Tax to analyze suppressive function of HBZ for the AP-1 pathway.[19,37] Therefore, this difference might be because of not only cell type, but also stimulator. HTLV-1 infects CD4 T cells and IFN-γ is

produced by stimulation of T cells, indicating that activation domain of HBZ plays an important role in suppression of AP-1 signaling.

The immune deficiency observed in ATL patients is one of the major factors in their poor prognosis. The mechanisms of HTLV-1–associated oncogenesis have been extensively investigated, yet there are only a limited number of reports regarding HTLV-1-related immune deficiency. Our results contribute to the understanding of this phenomenon by identifying a new mechanism of HTLV-1–induced immunodeficiency.

Acknowledgments

The authors thank T. Kitamura for the pMXs-Ig vector and Plat-E cells, H. Miyoshi for the pCS2-EF-GFP vector, T. Suzutani, Y. Koyanagi, and Y. Yoshikai for technical support in the HSV-2 studies, and L. Kingsbury for proofreading of the manuscript.

This work was supported by the Scientific Research from the Ministry of Education, Science, Sports, and Culture of Japan (Grant-in-aid), Novartis Foundation (M. Matsuoka), the Takeda Science Foundation, and the Naito Foundation.

Authorship

Contribution: K.S., Y.S., J.Y., H.H., M. Mitsuyama, and M. Matsuoka conceived and designed the experiments; K.S., Y.S., and K.O. performed the experiments; K.S., Y.S., J.Y., H.H., K.O., M. Mitsuyama, and M. Matsuoka analyzed the data; A.U. and M. Mitsuyama contributed reagents/materials/analysis tools; and K.S., Y.S., J.Y., M. Mitsuyama, and M. Matsuoka wrote the paper.

Conflict-of-interest disclosure: The authors declare no competing financial interests.

Correspondence: Masao Matsuoka, Laboratory of Virus Control, Institute for Virus Research, Kyoto University, 53 Shogoin Kawahara-cho, Sakyo-ku, Kyoto 606-8507, Japan; e-mail: mmatsuok@virus.kyoto-u.ac.jp.

References

1. Matsuoka M, Jeang KT. Human T-cell leukaemia virus type 1 (HTLV-1) infectivity and cellular transformation. *Nat Rev Cancer.* 2007;7(4):270-280.
2. Uchiyama T, Yodoi J, Sagawa K, Takatsuki K, Uchino H. Adult T-cell leukemia: clinical and hematologic features of 16 cases. *Blood.* 1977; 50(3):481-492.
3. Poiesz BJ, Ruscetti FW, Gazdar AF, Bunn PA, Minna JD, Gallo RC. Detection and isolation of type C retrovirus particles from fresh and cultured lymphocytes of a patient with cutaneous T-cell lymphoma. *Proc Natl Acad Sci U S A.* 1980; 77(12):7415-7419.
4. Hinuma Y, Nagata K, Hanaoka M, et al. Adult T-cell leukemia: antigen in an ATL cell line and detection of antibodies to the antigen in human sera. *Proc Natl Acad Sci U S A.* 1981;78(10): 6476-6480.
5. Gessain A, Barin F, Vernant JC, et al. Antibodies to human T-lymphotropic virus type-I in patients with tropical spastic paraparesis. *Lancet.* 1985; 2(8452):407-410.
6. Osame M, Usuku K, Izumo S, et al. HTLV-I associated myelopathy, a new clinical entity. *Lancet.* 1986;1(8488):1031-1032.
7. Sugimoto M, Nakashima H, Watanabe S, et al. T-lymphocyte alveolitis in HTLV-I-associated myelopathy. *Lancet.* 1987;2(8569):1220.
8. Takatsuki K, Matsuoka M, Yamaguchi K. ATL and HTLV-I-related diseases. In: Takatsuki K, ed. *Adult T-Cell Leukemia.* New York: Oxford University Press; 1994:1-27.
9. Cavrois M, Leclercq I, Gout O, Gessain A, Wain-Hobson S, Wattel E. Persistent oligoclonal expansion of human T-cell leukemia virus type 1-infected circulating cells in patients with tropical spastic paraparesis/HTLV-1-associated myelopathy. *Oncogene.* 1998;17(1):77-82.
10. Etoh K, Tamiya S, Yamaguchi K, et al. Persistent clonal proliferation of human T-lymphotropic virus type I-infected cells in vivo. *Cancer Res.* 1997; 57(21):4862-4867.
11. Nicot C, Harrod RL, Ciminale V, Franchini G. Human T-cell leukemia/lymphoma virus type 1 nonstructural genes and their functions. *Oncogene.* 2005;24(39):6026-6034.
12. Gaudray G, Gachon F, Basbous J, Biard-Piechaczyk M, Devaux C, Mesnard JM. The complementary strand of the human T-cell leukemia virus type 1 RNA genome encodes a bZIP transcription factor that down-regulates viral transcription. *J Virol.* 2002;76(24):12813-12822.
13. Satou Y, Yasunaga J, Yoshida M, Matsuoka M. HTLV-I basic leucine zipper factor gene mRNA supports proliferation of adult T cell leukemia cells. *Proc Natl Acad Sci U S A.* 2006;103(3):720-725.
14. Cavanagh MH, Landry S, Audet B, et al. HTLV-I antisense transcripts initiating in the 3′LTR are alternatively spliced and polyadenylated. *Retrovirology.* 2006;3:15.
15. Usui T, Yanagihara K, Tsukasaki K, et al. Characteristic expression of HTLV-1 basic zipper factor (HBZ) transcripts in HTLV-1 provirus-positive cells. *Retrovirology.* 2008;5:34.
16. Yoshida M, Satou Y, Yasunaga J, Fujisawa J, Matsuoka M. Transcriptional control of spliced and unspliced human T-cell leukemia virus type 1 bZIP factor (HBZ) gene. *J Virol.* 2008;82(19): 9359-9368.
17. Satou Y, Yasunaga J, Zhao T, et al. HTLV-1 bZIP factor induces T-cell lymphoma and systemic inflammation in vivo. *PLoS Pathog.* 2011;7(2): e1001274.
18. Zhao T, Yasunaga J, Satou Y, et al. Human T-cell leukemia virus type 1 bZIP factor selectively suppresses the classical pathway of NF-kappaB. *Blood.* 2009;113(12):2755-2764.
19. Basbous J, Arpin C, Gaudray G, Piechaczyk M, Devaux C, Mesnard JM. The HBZ factor of human T-cell leukemia virus type I dimerizes with transcription factors JunB and c-Jun and modulates their transcriptional activity. *J Biol Chem.* 2003;278(44):43620-43627.
20. Milligan GN, Bernstein DI, Bourne N. T lymphocytes are required for protection of the vaginal mucosae and sensory ganglia of immune mice against reinfection with herpes simplex virus type 2. *J Immunol.* 1998;160(12):6093-6100.
21. Iijima N, Linehan MM, Zamora M, et al. Dendritic cells and B cells maximize mucosal Th1 memory response to herpes simplex virus. *J Exp Med.* 2008;205(13):3041-3052.
22. Magee DM, Wing EJ. Cloned L3T4+ T lymphocytes protect mice against *Listeria monocytogenes* by secreting IFN-gamma. *J Immunol.* 1988;141(9):3203-3207.
23. Yang J, Kawamura I, Mitsuyama M. Requirement of the initial production of gamma interferon in the generation of protective immunity of mice against *Listeria monocytogenes*. *Infect Immun.* 1997; 65(1):72-77.
24. Iwamasa T, Utsumi Y, Sakuda H, et al. Two cases of necrotizing myelopathy associated with malignancy caused by herpes simplex virus type 2. *Acta Neuropathol.* 1989;78(3):252-257.
25. Ikehara O, Endo K, Hakamada K. Listeriosis in hematological malignancies: report of two cases. *Jpn J Clin Oncol.* 1989;19(2):159-162.
26. Suzutani T, Machida H, Sakuma T, Azuma M. Effects of various nucleosides on antiviral activity and metabolism of 1-beta-D-arabinofuranosyl-E-5-(2-bromovinyl)uracil against herpes simplex virus types 1 and 2. *Antimicrob Agents Chemother.* 1988;32(10):1547-1551.
27. Hara H, Kawamura I, Nomura T, Tominaga T, Tsuchiya K, Mitsuyama M. Cytolysin-dependent escape of the bacterium from the phagosome is required but not sufficient for induction of the Th1 immune response against *Listeria monocytogenes* infection: distinct role of Listeriolysin O determined by cytolysin gene replacement. *Infect Immun.* 2007;75(8):3791-3801.
28. Fan J, Kodama E, Koh Y, Nakao M, Matsuoka M. Halogenated thymidine analogues restore the expression of silenced genes without demethylation. *Cancer Res.* 2005;65(15):6927-6933.
29. Iwasaki A. Antiviral immune responses in the genital tract: clues for vaccines. *Nat Rev Immunol.* 2010;10(10):699-711.
30. Kaushic C, Ashkar AA, Reid LA, Rosenthal KL. Progesterone increases susceptibility and decreases immune responses to genital herpes infection. *J Virol.* 2003;77(8):4558-4565.
31. Unanue ER. Studies in listeriosis show the strong symbiosis between the innate cellular system and the T-cell response. *Immunol Rev.* 1997;158:11-25.
32. Ladel CH, Flesch IE, Arnoldi J, Kaufmann SH. Studies with MHC-deficient knock-out mice reveal impact of both MHC I- and MHC II-dependent T cell responses on *Listeria monocytogenes* infection. *J Immunol.* 1994;153(7):3116-3122.
33. Bettelli E, Dastrange M, Oukka M. Foxp3 interacts with nuclear factor of activated T cells and NF-kappa B to repress cytokine gene expression and effector functions of T helper cells. *Proc Natl Acad Sci U S A.* 2005;102(14):5138-5143.
34. Nakanishi K. Innate and acquired activation pathways in T cells. *Nat Immunol.* 2001;2(2):140-142.
35. Brown DA, Nelson FB, Reinherz EL, Diamond DJ. The human interferon-gamma gene contains an inducible promoter that can be transactivated by tax I and II. *Eur J Immunol.* 1991;21(8):1879-1885.
36. Hall WW, Fujii M. Deregulation of cell-signaling pathways in HTLV-1 infection. *Oncogene.* 2005; 24(39):5965-5975.
37. Matsumoto J, Ohshima T, Isono O, Shimotohno K. HTLV-1 HBZ suppresses AP-1 activity by impairing

both the DNA-binding ability and the stability of c-Jun protein. *Oncogene.* 2005;24(6):1001-1010.

38. Rouse BT, Sehrawat S. Immunity and immunopathology to viruses: what decides the outcome? *Nat Rev Immunol.* 2010;10(7):514-526.
39. Johnson JM, Nicot C, Fullen J, et al. Free major histocompatibility complex class I heavy chain is preferentially targeted for degradation by human T-cell leukemia/lymphotropic virus type 1 p12(I) protein. *J Virol.* 2001;75(13):6086-6094.
40. Sundstrom S, Ota S, Dimberg LY, Masucci MG, Bergqvist A. Hepatitis C virus core protein induces an anergic state characterized by decreased interleukin-2 production and perturbation of mitogen-activated protein kinase responses. *J Virol.* 2005;79(4):2230-2239.
41. Myskiw C, Arsenio J, van Bruggen R, Deschambault Y, Cao J. Vaccinia virus E3 suppresses expression of diverse cytokines through inhibition of the PKR, NF-kappaB, and IRF3 pathways. *J Virol.* 2009;83(13):6757-6768.
42. Li JC, Au KY, Fang JW, et al. HIV-1 trans-activator protein dysregulates IFN-gamma signaling and contributes to the suppression of autophagy induction. *AIDS.* 2011;25(1):15-25.
43. Li-Weber M, Krammer PH. Regulation of IL4 gene expression by T cells and therapeutic perspectives. *Nat Rev Immunol.* 2003;3(7):534-543.
44. Matsuoka M. HTLV-1 bZIP factor gene: its roles in HTLV-1 pathogenesis. *Mol Aspects Med.* 2010; 31(5):359-366.
45. Belkaid Y, Piccirillo CA, Mendez S, Shevach EM, Sacks DL. CD4+CD25+ regulatory T cells control Leishmania major persistence and immunity. *Nature.* 2002;420(6915):502-507.
46. Kursar M, Bonhagen K, Fensterle J, et al. Regulatory CD4+CD25+ T cells restrict memory CD8+ T cell responses. *J Exp Med.* 2002; 196(12):1585-1592.
47. Billiau A, Matthys P. Interferon-gamma: a historical perspective. *Cytokine Growth Factor Rev.* 2009;20(2):97-113.
48. Ungar BL, Kao TC, Burris JA, Finkelman FD. Cryptosporidium infection in an adult mouse model. Independent roles for IFN-gamma and CD4+ T lymphocytes in protective immunity. *J Immunol.* 1991;147(3):1014-1022.
49. Cenci E, Mencacci A, Del Sero G, et al. IFN-gamma is required for IL-12 responsiveness in mice with *Candida albicans* infection. *J Immunol.* 1998;161(7):3543-3550.
50. Sun JC, Bevan MJ. Defective CD8 T cell memory following acute infection without CD4 T cell help. *Science.* 2003;300(5617):339-342.

ACS Medicinal Chemistry Letters

LETTER

pubs.acs.org/acsmedchemlett

Potent CXCR4 Antagonists Containing Amidine Type Peptide Bond Isosteres

Eriko Inokuchi,[†] Shinya Oishi,*[,†] Tatsuhiko Kubo,[†] Hiroaki Ohno,[†] Kazuya Shimura,[‡] Masao Matsuoka,[‡] and Nobutaka Fujii*[,†]

[†]Graduate School of Pharmaceutical Sciences, Kyoto University, Sakyo-ku, Kyoto 606-8501, Japan

[‡]Institute for Virus Research, Kyoto University, Sakyo-ku, Kyoto 606-8507, Japan

Supporting Information

ABSTRACT: A series of FC131 [*cyclo*(-D-Tyr-Arg-Arg-Nal-Gly-)] analogues containing amidine type peptide bond isosteres were synthesized as selective CXC chemokine receptor type 4 (CXCR4) antagonists. An isosteric amidine substructure was constructed by a macrocyclization process using nitrile oxide-mediated C−N bond formation. All of the amidine-containing FC131 analogues exhibited potent SDF-1 binding inhibition to CXCR4. The Nal-Gly-substituted analogue was characterized as one of the most potent cyclic pentapeptide-based CXCR4 antagonists reported to date. The improved activity against human immunodeficiency virus (HIV) type-1 X4 strains suggested that addition of another basic amidine group to the peptide backbone effectively increases the selective binding of the peptides to CXCR4 receptor.

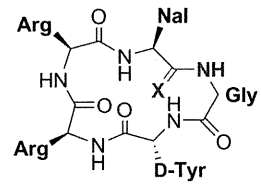

FC131: X = O;
IC_{50}(CXCR4) = 126 nM
EC_{50}(HIV-1) = 21 nM
15b: X = NH;
IC_{50}(CXCR4) = 4.2 nM
EC_{50}(HIV-1) = 1.4 nM

KEYWORDS: Amidine, chemokine, CXCR4 antagonist, FC131, nitrile oxide, peptidomimetics

CXC chemokine receptor type 4 (CXCR4) is a G protein-coupled receptor[1] for stromal cell-derived factor 1 (SDF-1)[2] that plays a critical role in the metastasis of mammary carcinoma[3] and in human immunodeficiency virus (HIV) type-1 infection.[4] CXCR4 is an important therapeutic target for these diseases.[5] To date, several types of CXCR4 antagonists with a variety of scaffolds have been reported (Figure 1).[6−11] Although the scaffolds of these antagonists have little in common, the antagonists all contain a number of basic groups. For example, the polyphemusin II-derived anti-HIV peptide, T140 **1**,[6] has seven basic Arg and Lys residues. Another example is the small molecule antagonist AMD3100, which contains eight secondary or tertiary amino nuclei.[7] Crystal structure analysis and mutation experiments of the receptor indicated that the ion-pairing interaction between the basic functional groups of the antagonists and the acidic residues in CXCR4 contributes to the potent bioactivity.[12−14]

FC131 [*cyclo*(-D-Tyr-Arg-Arg-Nal-Gly-), Nal = 3-(2-naphthyl)-alanine] **2** is a highly potent CXCR4 antagonist (Figure 1).[15] Using the peptide library approach, the potent anti-HIV activity of T140 **1** was reproduced with the appropriate arrangement of basic and aromatic residues on the cyclic pentapeptide framework of FC131. Further systematic structure−activity studies, such as alanine-scanning or amino acid optimizations, have been conducted to identify the structural and electrostatic requirements for the bioactivity of FC131.[16] Substitution of an Arg residue in **2** with the epimeric *N*-methyl-D-arginine led to identification of cyclic pentapeptide-based CXCR4 antagonist, FC122 **3**, which is the most potent CXCR4 antagonist among the FC131 derivatives reported to date.[16] However, backbone modification of **2** using peptide bond isosteres did not improve the bioactivity.[17−19] For example, replacement of several peptide bonds with reduced amide bonds **5** or alkene dipeptide isosteres **6** resulted in greatly reduced bioactivity (Figure 2), which suggests that these isosteric substructures are not appropriate for modifications of FC131. On the basis of these previous studies of FC131 derivatives and the common structural features of highly potent CXCR4 antagonists, we envisioned that addition of basic functional group(s) onto FC131 could improve its potency.

Recently, we established a novel synthetic approach for amidine type peptide bond isosteres **7** using nitrile oxide-mediated C−N bond formation.[20] Amidine type peptide bond isosteres were designed based on substitution of the peptide bond carbonyl (C=O) group with an imino (C=NH) group.[21,22] Under physiological conditions, the positive charge of the protonated amidines **7′** is delocalized over two nitrogens. Substructure **7′** contributes both the double bond character of peptide bond **4** and the basic character of reduced amide bond isostere **5′**. Therefore, the addition of this acyclic amidine group to the framework was expected to enhance the bioactivity without inducing large conformational change in the backbone structure. Accordingly, amidine-containing FC131 analogues **15a,b** and **15d−f** were designed, in which each peptide bond was replaced with the amidine substructure (Table 1). Compounds **15c** and **15g** were also designed as epimers of **15b** (at the Nal position) and **15f** (at the Tyr position), respectively. In this study, we investigated the contribution of amidine units to the bioactivity of amidine-containing FC131 analogues **15a−g**.

Received: February 15, 2011
Accepted: March 27, 2011
Published: March 28, 2011

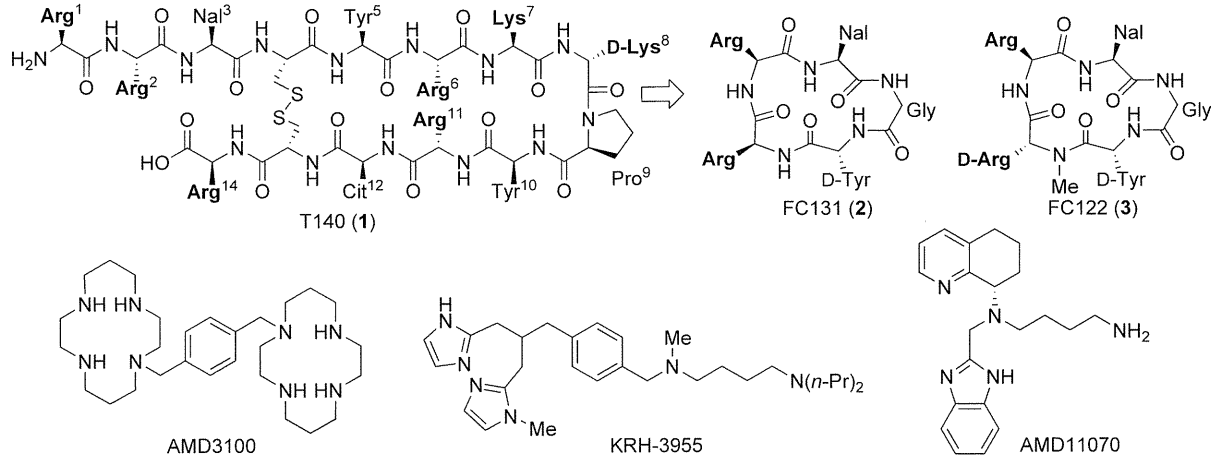

Figure 1. Structures of reported CXCR4 antagonists. Bold residues are basic residues. Nal = 3-(2-naphthyl)alanine.

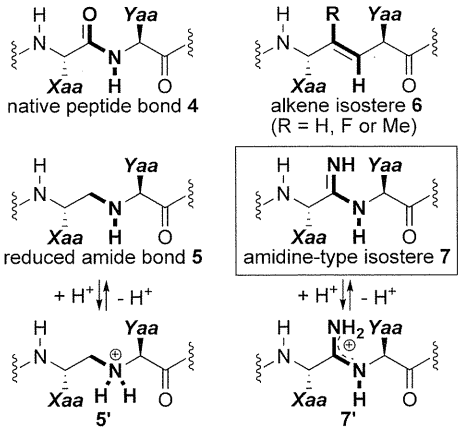

Figure 2. Structures of the peptide bond and the mimetics.

Table 1. Inhibitory Activity of FC131 and the Derivatives 15a–g against [^{125}I]-SDF-1 Binding to CXCR4

peptide	sequence[a]	IC_{50} (nM)[b]
FC131 (2)	*cyclo*(-D-Tyr-Arg-Arg-Nal-Gly-)	126 ± 68
FC122 (3)	*cyclo*(-D-Tyr-D-MeArg-Arg-Nal-Gly-)	37 ± 20
15a	*cyclo*(-D-Tyr-Arg-Arg-Nal-Gly-Ψ-)	9.4 ± 3.0
15b	*cyclo*(-D-Tyr-Arg-Arg-Nal-Ψ-Gly-)	4.2 ± 0.31
15c	*cyclo*(-D-Tyr-Arg-Arg-D-Nal-Ψ-Gly-)	4.9 ± 1.1
15d	*cyclo*(-D-Tyr-Arg-Arg-Ψ-Nal-Gly-)	11 ± 2.9
15e	*cyclo*(-D-Tyr-Arg-Ψ-Arg-Nal-Gly-)	16 ± 7.2
15f	*cyclo*(-D-Tyr-Ψ-Arg-Arg-Nal-Gly-)	679 ± 132
15g	*cyclo*(-Tyr-Ψ-Arg-Arg-Nal-Gly-)	334 ± 6.2

[a] Ψ indicates the ψ[−C(=NH)−NH−] substructure. Nal, 3-(2-naphthyl)alanine. [b] IC_{50} values are the concentrations for 50% inhibition of the [^{125}I]-SDF-1α binding to CXCR4 transfectant of HEK293 cells.

Synthesis of the L-Nal-Gly-substituted analogue **15b** is shown in Scheme 1 as a representative preparation of peptides **15a–g**. The first Nal residue was loaded onto aminooxy-2-chlorotrityl resin **8**[20] by treatment with Fmoc-3-(2-naphthyl)alaninal **9b** under acid-free conditions to give aldoxime resin **10b**. To prevent possible intramolecular cyclization between side chain guanidino and aldehyde groups in the preparation of aldoxime resins **10d** and **10e**, di-Boc-protected arginine [Arg(Boc)$_2$]-derived aldehyde was utilized for the preparation of Arg-Arg- and Arg-Nal-substituted analogues **15d** and **15e**. Peptide elongation was performed by the standard Fmoc-based solid-phase synthesis using *N,N'*-diisopropylcarbodiimide (DIC)/*N*-hydroxybenzotriazole (HOBt) in DMF. The cleavage of peptide aldoxime resin **11b** provided the linear peptide aldoxime **12b**, which was treated with *N*-chlorosuccinimide and triethylamine to afford cyclic amidoxime (*N*-hydroxyamidine) **13b**.[20] After Raney Ni-mediated reduction to the amidine **14b**, deprotection with a cocktail of 1M TMSBr, thioanisole/TFA, *m*-cresol, and 1,2-ethanedithiol gave the desired amidine-containing FC131 analogue **15b**. The analogues **15a** and **15c–g** were synthesized by the same procedure. During this nitrile oxide-mediated cyclization, significant epimerizations of the activated C termini of the peptides were not observed.[23]

The potency of the resulting FC131 analogues **15a–g** to inhibit [^{125}I]-SDF-1 binding to CXCR4 was evaluated (Table 1). Peptides **15a–e** were more potent than the control peptides **2** and **3**. This indicates that the basic amidine units had the expected effect of increasing the affinity with the receptor. By contrast, substitution of the Tyr-Arg dipeptide decreased the CXCR4 antagonistic activity (**15f** and **15g**). These observations were consistent with our previous study, in that the D-Tyr-Arg peptide bond is an indispensable functional group that is required to maintain the peptide conformation and the interaction with the receptor. Potent bioactivity of D-MeArg-substituted peptide (**3**) indicated that the amide hydrogen of Arg is not critical to the bioactivity,[16] while the local backbone conformation, particularly with respect to the orientation of D-Tyr carbonyl oxygen, may contribute to the receptor binding. Less potent bioactivity of **15f** and **15g** supports the significant contribution of D-Tyr carbonyl group in peptides **2** and **3**.

Nal-Gly-modified analogues **15b** and **15c** were the most potent inhibitors of the compounds synthesized in this study. At this Nal-Gly dipeptide position, the amidine substructure was more appropriate than the reduced amide motif (−CH_2−NH−), which exhibited slightly lower bioactivity than FC131 in our previous study.[17] It is interesting that modification at the Arg-Nal dipeptide (**15d**) gave potent bioactivity, whereas replacement of this dipeptide with the reduced amide bond in our earlier study reduced receptor binding.[17] This indicates that the high bioactivity of **15d** could be caused by conformational advantage rather than